

MEASUREMENT OF ABSOLUTE  $f$ -VALUES  
FOR SELECTED METALS BY THE  
ATOMIC BEAM METHOD

Thesis by

John Kailin Link

In Partial Fulfillment of the Requirements

For the Degree of

Doctor of Philosophy

California Institute of Technology

Pasadena, California

1963

## ACKNOWLEDGEMENTS

This experiment was part of a continuing project on the measurement of absolute  $f$ -values using the atomic beam method under the direction of Professor Robert B. King. I wish to acknowledge my appreciation for his generous advice and encouragement.

Mr. George M. Lawrence was responsible for the design of most of the new apparatus used in this work. Working closely with him has been a valuable educational experience for me.

The able assistance of Mr. Robert C. Ashenfelter in design and construction of electronic equipment has been valuable in the development of the new apparatus.

I wish to thank my wife, Ruth Link, for her steadfast work in the measurement of equivalent widths.

Finally, I would like to express my gratitude to the National Science Foundation for a fellowship during the years 1959-1962.

## ABSTRACT

Previous experimental work has demonstrated that the use of an atomic beam apparatus in the measurement of absolute  $f$ -values is a valuable method from which reliable experimental results can be obtained. Changes and improvements were made in the apparatus, increasing its sensitivity and reliability; these modifications are described.

A discussion of the validity of certain assumptions in the atomic beam theory is presented. A discussion is also presented of checks made on the reliability of the experimental measurements.

Absolute  $f$ -value measurements were made on the stronger resonance lines of Cr I, Ga I, In I, Tl I, Pd I, and Sn I. The results of these measurements are presented and compared with those of other investigators.

Suggestions are made for improvements in the atomic beam apparatus. These improvements would increase the number of elements whose absolute  $f$ -values could be measured by this method.

## TABLE OF CONTENTS

Part	Title	Page
I.	INTRODUCTION	1
II.	OUTLINE OF THEORY	6
III.	EXPERIMENTAL ANALYSIS AND TECHNIQUES	12
	A. Discussion of the Validity of the Atomic Beam Assumptions	15
	B. Optical System	17
	C. Vacuum System	20
	D. Crucibles and Furnace Tubes	24
	E. Microbalance	28
	F. Photomultiplier Detector	33
	G. Temperature Measurements	40
	H. Discussion of Errors	41
IV.	EXPERIMENTAL RESULTS	44
	A. Chromium I	45
	B. Gallium I	53
	C. Indium I	57
	D. Tin I	61
	E. Thallium I	64
	F. Palladium I	67
V.	DISCUSSION	70
	A. Absolute f-Values	70
	B. Relative f-Values	78
	C. Limitations of the Apparatus and Suggested Improvements	82
	D. Suggestions for Further Research	86

### LIST OF TABLES

Table	Title	Page
I.	Chromium I Data	51
II.	Gallium I Data	55
III.	Indium I Data	59
IV.	Tin I Data	62
V.	Thallium I Data	66
VI.	Palladium I Data	69
VII.	Absolute f-Values	76
VIII.	Relative f-Values	80

### LIST OF FIGURES

Figure	Title	Page
I.	Experimental Configuration	13
II.	Microbalance Output Tracings	29
III.	Hyperfine Structure Indium I, $\lambda 4101.76$	38
IV.	Photomultiplier Scanner Output Tracings	39
V.	Curve of Growth Chromium I, $\lambda 3578.69$	48
VI.	Impluse Force vs. Deposit Rate	49

## I. INTRODUCTION

The determination of transition probabilities, or  $f$ -values, for atomic electrons has been of interest to physicists even before the development of modern quantum theory.

The theoretical computation of these transition probabilities is severely limited by its dependency upon accurate wave functions for the initial and final electronic states. Accurate wave functions for atoms with more than one electron are very difficult to determine.

A number of techniques have been employed in the measurement of absolute  $f$ -values (1,2). Emission  $f$ -values obtained from arcs are unreliable because of the lack of precise knowledge of the temperature and emitting atom density within the arc plasma. Self-reversal of the emission lines constitutes an additional source of error. Physicists at the National Bureau of Standards (3) have investigated 25,000 lines in the arc spectra of seventy elements. Absolute and relative  $f$ -values obtained by other methods were used for calibration.

The measurement of the lifetime of an excited electronic state is a valuable experimental method for determining absolute  $f$ -values if the relative  $f$ -values of all the possible transitions from the excited state are known. Recent experiments conducted in Germany have utilized this method (4,5).

The determination of f-values by the analysis of spectral lines formed in absorption has certain advantages over the use of emission lines: the condition of atoms in the absorbing gas is relatively simple to describe theoretically as well as to control experimentally. Professor R. B. King and his co-workers have determined, through use of the King furnace, relative f-values for most of the elements between titanium and nickel on the periodic table. Absorption lines were formed when light from a continuous source was sent through monatomic vapour of the element being studied (6,7).

If the vapour pressure of the element is known as a function of temperature, and if the absorbing vapour is in thermal equilibrium, it is then possible to measure absolute f-values. Quartz cells have been used to confine metal vapours in such a state of equilibrium<sup>(8)</sup>. This technique has been unreliable, however, since much of the vapour pressure data were in error by at least fifty percent (9,10).

The relative f-values for lines of an element can be determined by measuring the anomalous dispersion of its vapour in the immediate vicinity of each absorption line. This method has been widely used in the Soviet Union (11,12,13). If the vapour is maintained in a state of thermal equilibrium, the relative f-values can be converted to an absolute scale by using vapour pressure data.

The atomic beam method was first introduced by Kopfermann and Wessel (14,15). The following experimentalists

have done much work on improving the techniques and in verifying the reliability of the method: M. H. Davis (16) P. M. Routly, and G. D. Bell (17), under the supervision of Professor King. Their work has resulted in the publication of absolute  $f$ -values for Cu I, Fe I, Mn I, and Pb I (18, 19, 20).

The experiment described in this thesis used an atomic beam apparatus. A small, chemically pure sample of the metal being studied was placed in a crucible with which it would not react chemically. The metal was heated to a temperature at which its vapour pressure was approximately .02 Torr. A small percentage of the atoms in the crucible effused from an orifice in the side, forming an atomic beam. The beam was fan-shaped because of knife edges which defined its opening angle. The atomic beam entered a vacuum chamber in which the pressure was between  $3 \times 10^{-6}$  and  $5 \times 10^{-7}$  Torr.

Quartz windows on either side of the vacuum chamber allowed light, from a high pressure mercury discharge lamp, to pass through the atomic beam in a form approximating a flat horizontal sheet. The absorption line thus formed was scanned with a high resolution, high gain, photomultiplier scanner placed in the camera holder of a 22 foot Rowland mounting spectrograph. The output of the scanner after filtering, amplification, and zero shifting was traced on a strip chart recorder. The equivalent width (or total absorption of the line) was then obtained by

measuring the area under the line profile traced upon the strip chart.

While the absorption line was being scanned, a second strip chart recorder was continuously marking the rate at which atoms in the atomic beam were deposited onto a microbalance pan. That part of the atomic beam which impinged upon the microbalance pan was determined by a circular aperture directly above the opening in the crucible. The temperature at the inside of the crucible was measured with an optical pyrometer. From a knowledge of the geometry, the temperature inside the crucible, and the rate at which the atomic beam deposited onto the microbalance pan, it was possible to compute the actual density of absorbing atoms integrated along the path of the light beam. After determining the above quantities, the  $f$ -value of the line being studied could then be calculated by relating the equivalent width to the concentration of absorbing atoms.

The work of G. D. Bell (17) showed that the assumptions involved in determining atomic beam densities from beam geometry, crucible temperature, and deposit rate on the microbalance pan were justified; on the other hand, this work indicated a need for a more sensitive and accurate determination of both equivalent widths and deposit rates. A considerable amount of time was spent, therefore, in close collaboration with G. M. Lawrence (21) in making the desired improvements.

A brief discussion of the newly developed apparatus will follow. Results are given for 25 accessible resonance lines of Cr I, Sn I, Pd I, Ga I, In I, and Tl I; comparisons are then made with the work of other investigators. However, a resumé will first be presented outlining the theory necessary to define the quantities used in the experimental analysis.

## II. OUTLINE OF THEORY

The general theory for the formation of absorption lines in a monatomic gas is well understood. Useful references are Unsöld (1) and Aller (22). Davis (16) has developed the modifications necessary for the analysis of lines formed in absorption from an atomic beam.

The equivalent width of a line is a useful parameter in describing its strength:

$$W_{\epsilon} = \int \frac{I_0 - I_{\lambda}}{I_0} d\lambda .$$

$I_0$  is the continuum intensity in the absence of absorption, and  $I_{\lambda}$  is the intensity as a function of wavelength in the presence of absorption. As defined here, the equivalent width is the equivalent amount of the continuum, in wavelength units, which is totally absorbed in the formation of the line.

Line formation theory states, for the case of pure doppler broadening ( $\Delta\lambda_n/\Delta\lambda_D \ll 1$ , where  $\Delta\lambda_n$  is the natural width of the line and  $\Delta\lambda_D$  is the doppler width), that

$$\frac{W_{\epsilon}}{\Delta\lambda_D} = H \left( K \cdot \frac{NfL}{\Delta\lambda_D} \right) \quad (1)$$

where  $f$  is the  $f$ -value for the line,  $N$  is the density of absorbing atoms in the light path,  $L$  is the optical path length, and  $K$  is a constant for a given line. This relation is known as the curve of growth and can be obtained explicitly in terms of an infinite series. When  $W_{\epsilon}/\Delta\lambda_D < .4$ , the

first term in the series makes the major contribution; the relation then becomes linear.

In developing the theory for the atomic beam the following assumptions are made:

1. The pressure in the vacuum system is low enough so that less than one percent of the atoms in the beam will collide with residual gas molecules in travelling the three inch distance between the crucible orifice and the microbalance pan.

2. The atoms of metal vapour reach thermal equilibrium inside the crucible. The presence of the hole in the crucible does not significantly effect this equilibrium condition; in other words, the mean free path of atoms in the crucible is large compared to the size of the orifice.

3. The crucible orifice is small enough to be considered a point source when viewed from a distance of 1.5 inches or more.

4. The changes in weight of the microbalance pan are due only to the deposit of atoms from the atomic beam. All incident atoms stick to the pan.

Davis <sup>(16)</sup> obtained the following expression as the explicit form which equation 1 takes in the atomic beam case:

$$\frac{W_E}{\Delta \lambda'_D} = \sqrt{\pi} \sum_{n=1}^{\infty} \frac{C^n (-1)^{n+1}}{n! \sqrt{n}} \cdot \quad (2)$$

In this expression,  $\Delta \lambda'_D$  is an effective doppler width

appropriate to the velocity distribution in the atomic beam, and C is proportional to  $NfL/\sqrt{T}$  of the atomic beam.

The quantities in equation 2 are defined as follows:

$$\Delta \lambda'_D = .430 \lambda_0 \sqrt{\frac{T}{M}} \sin \gamma, \quad (3)$$

$\lambda_0$  is the wavelength of the line in units of  $10^{-5}$  cm, T is the crucible temperature in degrees Kelvin, M is the mass of the element in atomic mass units, and  $\gamma$  is the half angle of the atomic beam. If the quantities in equation 3 are expressed in these units, then  $\Delta \lambda'_D$  will be in milliangstroms.

Continuing with a definition of the quantities in equation 2,

$$C = \frac{fG'}{QT}, \quad (4)$$

$$\text{where } Q = 8.33 \times 10^{-3} \cdot \frac{Z}{\lambda} \frac{P^2}{b^2 + P^2}; \quad (5)$$

Z is the distance, in inches, above the crucible orifice at which the light beam passes through the atomic beam; b is the vertical distance from the crucible orifice to the circular aperture, defining that part of the atomic beam which strikes the microbalance pan; and P is the radius of this circular aperture.  $G'$  is the rate at which atoms capable of absorbing a photon of the wavelength of the spectral line deposit on the microbalance pan.  $G'$  is measured in micrograms per second and is related to G, the observed deposit rate, by a Boltzman factor describing the

distribution of atoms over the low lying energy levels of the atom. Accordingly,  $G' = (\text{B.F.})G$  where

$$\text{B.F.} = \frac{g_i e^{-\frac{E_i}{RT}}}{\sum_j g_j e^{-\frac{E_j}{RT}}} \quad (6)$$

The quantity  $g_1$  is  $2J+1$  for the lower state of the transition, and  $E_1$  is its energy. The sum extends over all low lying states which have an appreciable population at the temperature of the crucible.

A complication arises when the line under investigation has hyperfine structure components separated by more than  $.5 \text{ m}\text{\AA}^\circ$  (23). If the separation of the components is smaller than the effective doppler width of the line, the blending of the components is quite complicated, and the equivalent width should be kept small ( $W_E/\Delta\lambda'_D < .4$ ) so that the line is on the linear part of the curve of growth where

$$\frac{W_E}{\Delta\lambda'_D} = \sqrt{\pi} C. \quad (7)$$

When the splitting of the hyperfine structure components is greater than or equal to the effective doppler width of the line, but unresolved by the spectrograph, the components are blended and each component follows a separate curve of growth:

$$\frac{W_E)_i}{\Delta\lambda'_D} = H(C_i).$$

Values of  $C_1$  have relative magnitudes given by the theoretical relative intensities of the hyperfine structure

components. These theoretical relative intensities can be obtained from the tables of White and Eliason (24) if the nuclear spin and J values for the upper and lower terms are known.

In practice,  $(W_{\epsilon}/\Delta\lambda'_{D})_{T_{\epsilon}}$  for the unresolved line, the relative values of the  $C_1$ , and tabulated values for the curve of growth function for a single component are known and the theoretical curve of growth for the unresolved line, relating  $(W_{\epsilon}/\Delta\lambda'_{D})_{T_{\epsilon}}$  to  $C_{total}$ , is desired. A series of  $C_{total}$  values covering the range of experimental interest were selected. Each  $C_{total}$  was then expressed as a sum of  $C_1$ ,  $C_{total} = \sum_i C_1$ , where the  $C_1$  have the correct relative values for the line being studied. For each  $C_1$ , a  $(W_{\epsilon_i}/\Delta\lambda'_D)$  was obtained:

$$\frac{W_{\epsilon_i}}{\Delta\lambda'_D} = H(C_i).$$

The composite curve of growth was a graph of  $C_{total}$  against  $(W_{\epsilon}/\Delta\lambda'_{D})_{Total}$  where

$$\left. \frac{W_{\epsilon}}{\Delta\lambda'_D} \right)_{Total} = \sum_i \frac{W_{\epsilon_i}}{\Delta\lambda'_D}.$$

Using the quantities defined above, the absolute f-value for the line was then obtained from the equation:

$$f = \frac{QCT}{G}. \quad (8)$$

A final relation, derived by Davis<sup>(16)</sup>, for the impulse force received by the microbalance pan upon opening the shutter is very useful in analyzing the meaning of

the tracings from the automatically balancing microbalance:  
 $F = t_r G$ .  $F$  is the impulse force in micrograms and  $t_r$  is  
the time necessary to deposit a mass with weight equal to  
 $F$ . The recovery ( $t_r$ ) can be computed from the following  
equation:

$$t_r = 17.5 \sqrt{T/M} .$$

### III. EXPERIMENTAL ANALYSIS AND TECHNIQUES

The experimental methods used to measure absolute  $f$ -values will be described in some detail in the following eight sections. Aspects of the experimental apparatus which are not fully described have already been discussed in detail by Davis (16) and Bell (17).

Figure I shows a schematic drawing of part of the apparatus. A crucible (1) is shown properly positioned in a furnace tube (2). The furnace tube is slipped snugly into high current electrodes, which are water cooled. The power source is capable of providing an input power of over 2 kw. at currents of several hundred amps. The knife edges (3) define the angular spread  $\gamma$  of the atomic beam. The aperture (4) admits a portion of the atomic beam to the microbalance pan. A shutter (5) shields the microbalance pan, and (7) indicates the calibrating hook on which the standard weight for calibrating the balance is placed.

A schematic drawing of the automatic balancing mechanism is centered around (8) in figure I. The balance coil is suspended by taut .001 in. tungsten wires in the field of a permanent magnet. The balance arm from which the pan is suspended is rigidly attached to the balance coil. A small focusing light bulb directs light toward two photocells. A flag attached to the balance arm blocks some of this light. The automatic balancing circuit adjusts the

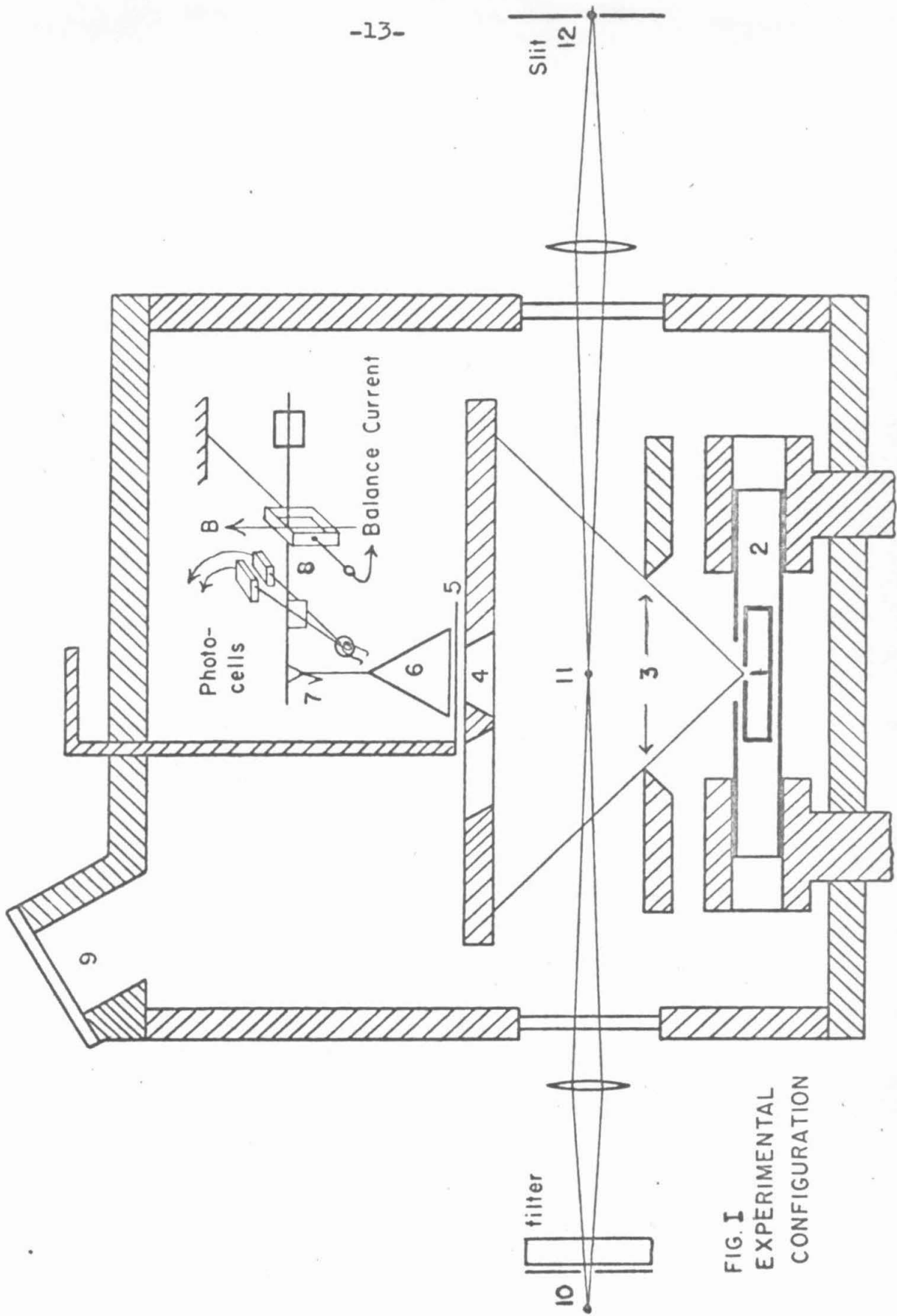


FIG. I  
EXPERIMENTAL  
CONFIGURATION

current through the balance coil until the output signals from the two photocells are equal.

The temperature of the crucible orifice is measured with an optical pyrometer by viewing through the window (9). A rotatable quartz disc underneath the window protects it from fogging by the atomic beam.

The high pressure mercury discharge light source is located at (10). The light from the lamp is imaged at the center of the atomic beam (11) and then re-imaged on the entrance slit of the spectrograph (12).

A. Discussion of the Validity of the Atomic Beam Assumptions

The geometrical distribution of the atomic beam was checked by Bell (17) and found to agree, to within experimental error, with that predicted by assuming effusive flow from a point source.

The velocity distribution of the atoms in the atomic beam can be calculated from the temperature of the vapour inside the crucible using kinetic theory for effusive flow, provided the mean free path of the atoms inside the crucible is long compared to the dimensions of the orifice. To determine the validity of the assumption of effusive flow, mean free paths ( $\lambda$ ) were computed for the temperatures used in vapourizing chromium. Vapour pressures for chromium were taken from the tables given by Stull and Sinke (25).

The extreme values are reported here:

$$T = 1963 \text{ }^\circ\text{K}$$

$$\lambda = 0.8 \text{ mm.}$$

$$G = 1.2 \text{ } \mu\text{gm/sec}$$

$$T = 1700 \text{ }^\circ\text{K}$$

$$\lambda = 26 \text{ mm.}$$

$$G = .045 \text{ } \mu\text{gm/sec}$$

The diameter of the crucible orifice was about 1 mm. The mean free paths of all the other elements studied, except tin and indium, fell within the range given above.

For tin and indium, lines from excited states with f-values less than .05 were studied. The beam densities which were necessary to produce measurable absorption lines led to mean free paths of less than .3 mm. inside the crucibles, when standard graphite crucibles with .04 in.

diameter orifices were used. To check on the effect of these short mean free paths on the measured  $f$ -values special crucibles with orifices .11 in. in diameter were used in repeating the measurements on two  $f$ -values of tin and two  $f$ -values of indium. The repeated  $f$ -values agreed with those obtained using standard crucibles to less than 5%. The mean free paths inside the special crucibles were always greater than 3 mm.

Thus, the restrictions imposed by the assumption of effusive flow do not seem to have been violated in the experimental work reported in this thesis.

### B. Optical System

A high pressure mercury discharge lamp was used as a light source. It had a high intensity output and lifetime of about 50 hours, while operating with an input power of 1.1 kw., as long as a steady flow of cooling water was maintained to carry off the heat generated. Both the capillary, which contained the mercury, and the outer water jacket of the lamp were made of quartz to allow transmission of light with wavelength shorter than  $3000 \text{ \AA}$ . During operation of the lamp, the pressure inside the capillary rose to several hundred atmospheres. The mercury emission lines were, therefore, extremely pressure broadened. The lamp output was a useful source from  $2650 \text{ \AA}$  to at least  $7000 \text{ \AA}$ . Below  $2650 \text{ \AA}$  the self absorption of the mercury  $2536 \text{ \AA}$  line drastically reduced the light output. Near the mercury emission lines the continuum intensity varied at least a factor of ten.

The mercury lamp was placed in a horizontal position, and a quartz lens with 15 cm. focal length was used to bring the line image of the capillary to focus in the center of the atomic beam. A 30 cm. focal length quartz lens then focused this image on the entrance slit of the spectrograph. This simple optical system was designed by G. M. Lawrence to admit a maximum amount of light to the spectrograph by filling both the length and breadth of the entrance slit. Both lenses were mounted on precision lens mounts, which allowed fine adjustments of the optical alignment to be made.

Light was admitted into the vacuum system through optical quartz windows sealed to the main vacuum chamber by means of O-rings.

The large Rowland mounting spectrograph, located in Bridge Laboratory, was used for this experiment. The 21 foot grating used in the thesis work of both Bell and Davis had been replaced because of the large amount of scattered light it produced. The grating used for the work reported in this thesis had a radius of curvature of 6650 mm., 600 rulings per mm., and a ruled area 5 cm. by 12 cm. All work was done in second order, where the dispersion was 1.252  $\text{A}^\circ/\text{mm}$ .

The following simple test was made for the presence of scattered light by the new grating. The chromium  $\lambda 3578$  line was scanned six times, using the second order of the spectrograph, with a Corning glass filter blocking out all light of wavelength longer than 3900  $\text{A}^\circ$ . The filter was removed, and the line was scanned six more times. This was possible because the EMI 9526B photomultiplier was insensitive to the first order light of 7150  $\text{A}^\circ$ , and the mercury discharge lamp emits virtually no third order light of wavelength 2380  $\text{A}^\circ$ . The crucible temperature was constant during these scans. The resulting f-values, calculated for the chromium  $\lambda 3578$  line, did not differ significantly from each other, thus indicating that the presence of scattered light was not a problem at 3578  $\text{A}^\circ$ .

A Corning glass filter, "Red Purple Corex-A", was used to separate orders of the spectrograph in the wavelength region between  $2700 \text{ \AA}$  and  $3650 \text{ \AA}$ . For the wavelength region  $3650 \text{ \AA}$  to  $5000 \text{ \AA}$ , a Corning glass "Furnace Door Blue" filter was used.

### C. Vacuum System

The vacuum system was originally designed to attain a pressure low enough that less than 1% of the atoms in the atomic beam would suffer collisions with the residual gas in the system. The distance between the crucible orifice and the microbalance pan was 7 cm. Using kinetic theory, the following expression has been derived for the fraction,  $\alpha$ , of atoms in the atomic beam suffering collisions in traveling a distance Z (in cm.) at a residual gas pressure P (in  $10^{-3}$  Torr):  $\alpha = ZP/6.5$ . For Z = 7 cm., this expression becomes  $\alpha = 1.1P$ . Thus, at pressures below  $10^{-5}$  Torr, less than 1% of the atoms in the atomic beam will collide with residual gas atoms in traveling from the crucible to the microbalance pan.

Observation of the instantaneous weight of the microbalance pan under conditions of atomic beam deposition indicated that gettering, adsorption, and liberation of gas by the pan could very adversely effect the accuracy of the deposit rate determinations. The conical aluminum foil pans used throughout this work had a total surface area of approximately  $20 \text{ cm}^2$ . Deposit rates observed during the measurement process ranged from .02 to 2 micrograms per second. The following expression was obtained from kinetic theory for R, the rate of mass incidence in micrograms per  $\text{cm}^2$  per second, as a function of pressure for a residual gas of pure nitrogen, at  $30^\circ\text{C}$ :  $R = .016P$ ,

where  $P$  is expressed in  $10^{-6}$  Torr. For the pans used in this experiment the expression becomes  $R = .32P$ . At a residual gas pressure of  $10^{-9}$  Torr, the mass incidence rate becomes  $.0003 \mu\text{gm}/\text{sec.}$ , which is about 1% of the lowest observed atomic beam deposit rates. At the gas pressure of  $10^{-6}$  Torr, commonly obtained during actual atomic beam deposition,  $R$  was therefore about  $.3 \mu\text{gm}/\text{sec.}$

The composition of the residual gas in the vacuum system at  $10^{-6}$  Torr probably differed quite drastically from that of air. Nitrogen and cracked pump oil fragments such as methane and carbon monoxide were the main components. The chemical reactions that could occur between these residual gas components and fresh, chemically active, deposits on the microbalance surface are quite complicated. The metals studied in this thesis are not very active chemically and there was no evidence of such reactions.

The nature of the experimental work being done with the vacuum system required that it be readily demountable to allow for frequent refilling of the crucible and measurement of the quantities determining the atomic beam geometry. The system designed by Davis <sup>(16)</sup> and Routly had O-ring seals and many ports to provide easy access to the inside of the system. The pumping system consisted of a 4 in. Kinney fractionating oil diffusion pump backed by a two stage 5 cu. ft./min. Kinney mechanical pump. This pumping system should attain a minimum pressure of  $2 \times 10^{-6}$  Torr.

To improve the ultimate vacuum attainable, a large liquid nitrogen cold trap with a lifetime of about 4 hours was placed in the baffle valve above the throat of the diffusion pump. This location was chosen to reduce as much as possible the back-streaming of diffusion pump oil into the vacuum system. The ultimate pressure of the system with the cold trap was about  $10^{-7}$  Torr.

Viton, a fluorine-carbon compound with elastic properties, makes O-rings which are superior to those made of buna rubber because of viton's lower vapour pressure and ability to withstand temperatures of  $100^{\circ}\text{C}$ . The vacuum system had 30 buna rubber O-rings seals, which were replaced with seals made of viton.

The vacuum pressure gauge installed by Bell was a CVC Phillips gauge capable of measuring pressure accurately down to  $10^{-6}$  Torr. A Veeco non-burnout ionization gauge with a linear output and a sensitivity of  $100 \mu\text{amps}$  per  $10^{-3}$  Torr at 10 mA grid current was added to the system, providing accurate pressure reading below  $10^{-6}$  Torr.

With the viton O-rings, the lowest pressure attained in the main vacuum chamber was  $2 \times 10^{-7}$  Torr. An attempt was made to drive off absorbed gas and thereby speed pump-down time by heating the outside walls of the vacuum chamber to  $90^{\circ}\text{C}$ . This was soon abandoned because the heat caused the viton O-rings to take on a permanent set and the ultimate pressure was not lowered. The pump-down time, without heating of the walls of the vacuum chamber,

was about 24 hours.

The ultimate attainable pressure of the pumping system was checked by putting the Veeco Gauge directly on the input port leading to the diffusion pump and pumping on the closed port. The pressure thus measured was not significantly lower than that attained while pumping on the entire vacuum chamber. Therefore, it was concluded that the pump itself was the limiting factor and not out-gassing of the chamber or leaks through the O-rings.

The pressure while the furnace was operating was usually a factor of ten above the minimum attainable pressure when the furnace was cold. This was especially true with palladium, which required crucible temperatures of about 1850 °C and, therefore, furnace tube temperatures of over 2000 °C. The rise in pressure while the furnace was hot was attributed to out-gassing of the inside of the system because of exposure to heat and radiation from the furnace. In principle, this out-gassing should stop if the furnace were maintained at elevated temperatures for a period of hours; however, such a long out-gassing period would exhaust the supply of metal in the crucible. It was found that maintaining the furnace for several hours at a temperature just below that at which the element in the crucible attained an appreciable vapour pressure helped to reduce the pressure at the higher temperature used to produce the atomic beam.

D. Crucibles and Furnace Tubes

Graphite, because of its excellent thermal shock resistance, was used for vapourizing any element with which it did not react chemically. The graphite crucibles used for this work were machined from pure spectroscopic graphite rods. They were 1.3 in. long, had an outer diameter of .352 in., and a wall thickness of .018 in. Snugly fitting caps were machined for the open ends, and holes with .045 in. diameters were drilled in the sides in order to allow formation of the atomic beam. The crucibles were made with little "ears" to hold them away from the furnace tubes, and to thus prevent an excess amount of current from passing through the crucible.

Graphite furnace tubes were used with the graphite crucibles. These were 3.5 in. long, with an outer diameter of .453 in., and a wall thickness of .033 in. A hole .150 in. in diameter was drilled in their sides. This hole was made just large enough so that it would not interfere with the atomic beam. It was felt that having the hole as small as possible was desirable in order to reduce the cooling of the area of the crucible near the hole, and to thus reduce the amount of metal vapour condensing there. Deposition of metal around the orifice caused variations in the observed deposit rates.

Unfortunately, elements in the immediate vicinity of iron on the periodic table form carbides upon melting in

graphite containers. Bell (17) found that stabilized zirconium oxide had the necessary chemical inertness to contain molten metals in the iron group. Zirconia, however, does not have the excellent thermal shock resistance of graphite; and after being used once to produce an atomic beam, a crucible would be too cracked for reuse.

The zirconia crucibles used for this work were obtained from the Leco Company in St. Joseph, Michigan. These were 1 in. in length and were closed at one end. The outer diameter was .375 in. and the wall thickness was .094 in. The Leco Company did not supply plugs for the open ends, so a technique was devised to produce them. Stabilized zirconium oxide was mixed with polystyrene cement diluted with benzene to form a thick paste. The paste was then packed into molds, which were drilled out of .250 in. brass sheet. After allowing the benzene to evaporate, the full mold was heated with a cool acetylene torch so that the polystyrene would burn out. Using a hotter torch, the whole mold was heated until the brass melted and rolled free of the zirconia plug. Finally, the plug was sintered by heating it to white heat with the hottest part of the acetylene flame. This technique produced impervious plugs, which closed the open ends of the crucibles very effectively.

The holes from which the atomic beam was formed were ground in the sides of the zirconia crucibles with a soft wheel.

At first, graphite tubes were used with the zirconia crucibles, but it was found that large amounts of gas evolved upon reaching furnace temperatures in excess of 1800 °C. This was attributed to a reaction between the zirconia and the graphite, which liberated oxygen. Next, furnace tubes rolled out of .003 in. molybdenum were tried, but it was found that they developed hot spots and burned out at temperatures above about 1700 °C. It was finally found that .005 in. tantalum made very satisfactory tubes, which neither burned out nor evolved gas. The tantalum tubes were 4 in. in length with .310 in. diameter holes punched in the sides for the passage of the atomic beam. The larger holes in the side of the tantalum tubes were necessary to allow clearance for the atomic beam. Unfortunately, this meant that the area around the crucible opening was differentially cooled because of radiation losses, thus causing some deposition of metal around the orifice. A chemical reaction between the zirconia crucibles and the tantalum heating tubes was observed, which produced a weakening of the tantalum at points of contact. This was eliminated by wrapping the bottom half of the crucible with a patch of tantalum .005 in. thick, in order to prevent any direct contact between the crucible and the furnace tube.

A set of concentric radiation shields, spot welded out of .005 in. tantalum, reduced the input power requirements necessary to reach temperatures above 1600 °C. The

radiation shields were isolated from each other and the furnace tube, both thermally and electrically, by means of annular spacers cut from quartz tubing of the appropriate size. It was found that the triple radiation shield cut the input power necessary to reach temperatures above 1600 °C in the crucible by at least a factor of two.

A test run was made with an empty zirconia crucible in a tantalum furnace tube in order to determine the highest attainable crucible temperature. At about 2200 °C the zirconia melted and reacted with the furnace tube causing it to burn out.

### E. The Microbalance

The automatically balancing microbalance used in this experiment was designed by G. M. Lawrence <sup>(21)</sup> and R. C. Ashenfelter. The sensitivity of the balance was about .4  $\mu\text{gm.}$ , and it had a dynamic range of 5 mgm. The balance was calibrated by weighing a standard 1 mgm. rider in vacuo. This calibration was assumed to hold for much smaller changes in weight because the automatic balancing mechanism always brought the balance to rest in the same position. For the experimental work reported in this thesis, deposit rates on the balance pan were in the range from .03 to 1.5  $\mu\text{gm./sec.}$  The aperture which allowed the atomic beam to deposit on the microbalance pan was .576 in. in diameter. For elements with f-values below .05, where high beam densities were needed, a plug with a .376 in. hole in its center was placed over the larger aperture.

Figure II shows two tracings of actual microbalance strip chart recordings. With the shutter under the microbalance closed, the balance reads a constant weight. Upon opening the shutter an upward impulse, due to the arrival of the atomic beam, makes the pan seem lighter. Deposition of mass is marked by a steady increase in the weight of the pan. The recorder tracing should be nearly a straight line for a constant deposit rate. Runs where the deposit rate was clearly not constant were rejected. Three obvious causes of variation in deposit rate were: fluctuating

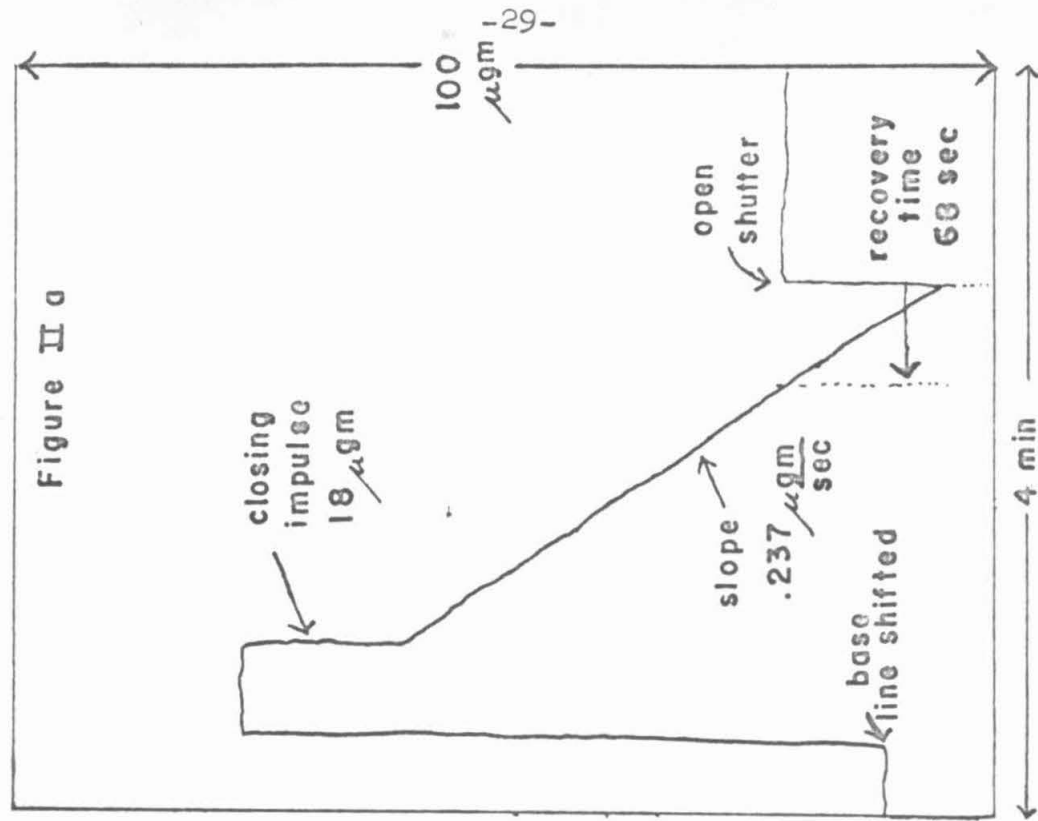
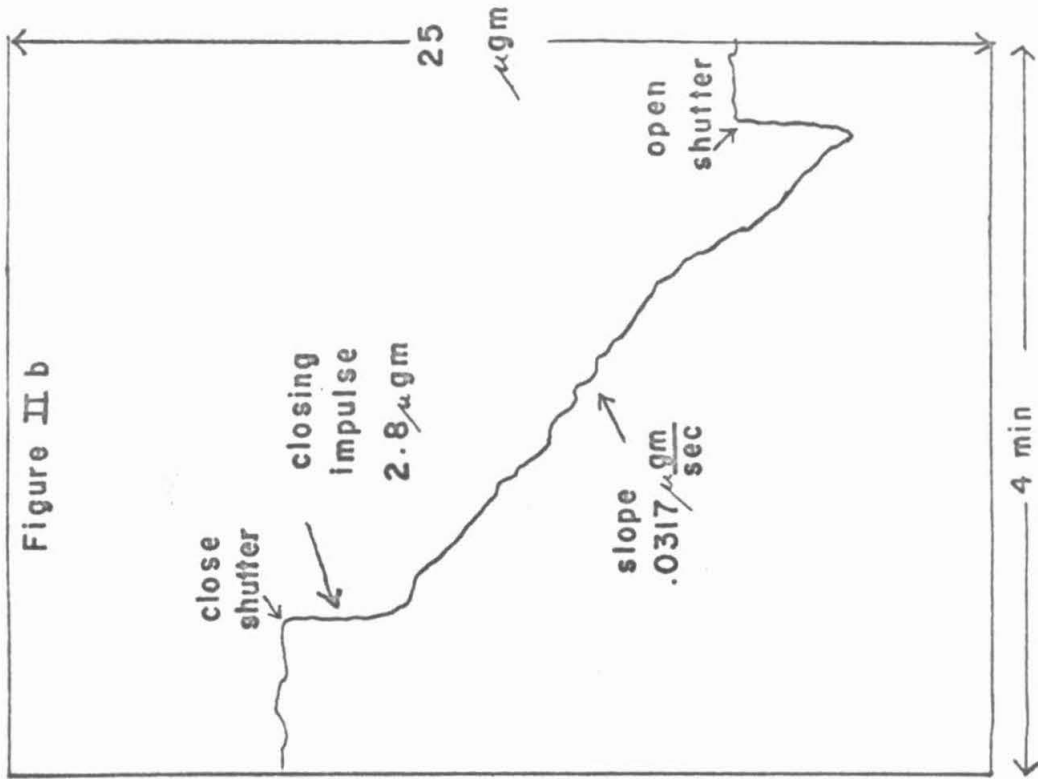


FIGURE II REPRESENTATIVE MICROBALANCE OUTPUT TRACINGS

crucible temperature, formation or disappearance of deposits about the crucible orifice, and exhaustion of the material inside the crucible.

Figure II b shows a deposit rate of about  $.03 \mu\text{gm./sec.}$  The non-linearity of the tracing is due to the low deposit rate, which is at the lower limit of the useful range of the balance. The noise level in the balance is shown by the irregularity in the tracing in Figure II b when the shutter was closed. Figure II a shows how the recovery time,  $t_r = 17.5\sqrt{T/M}$ , can be read off the output chart as a horizontal distance between points on the time scale when the microbalance records equal weights.

Pans for the balance were made from .00025 in. thick aluminum foil. A quarter sector of a 1.6 in. radius disc cut from the foil was shaped around a conical form and spot welded into a conical pan. Conical pans were used because a large fraction of the atoms which bounced off the pan surface on the first encounter would have to hit the pan at least once more before escaping. Therefore, the fraction of atoms finally sticking to the conical pan would be much higher than the fraction sticking after a single encounter.

As much as  $100 \mu\text{gm.}$  of gas were observed to leave a pan when it was first exposed to radiation from the furnace. A small six volt tungsten light bulb was placed near the balance pan to heat it and drive off this absorbed gas. It was often found that even when pans were heated they

absorbed some gas, though at a much slower rate than unheated pans. The rate of gas absorption was found to be highest right after a fresh layer of metal atoms had been deposited on the pan. Heated pans apparently accumulated a thin surface layer of gas atoms on top of the fresh deposit. When the shutter was opened again this small amount of absorbed gas, generally less than 2  $\mu\text{gm.}$ , was driven off by exposure to the furnace in less than ten seconds. Part IV section A contains a discussion of gas absorption observed on fresh chromium deposits.

The rapid evolution of gas made it difficult to obtain an accurate impulse force measurement when the shutter was opened. It was found that the impulse force measurement, obtained when the shutter was closed, was more reliable because of the absence of this effect.

The motion of the residual gas in the vacuum chamber toward the input port of the diffusion pump produced a noticeable wind at pressures above  $10^{-5}$  Torr. The pan would appear to get heavier when the shutter, directly beneath it, was opened.

When the region around the furnace was evolving gas because of a sudden increase in furnace temperature, an upward wind was often observed. This wind made the microbalance pan appear lighter upon opening of the shutter.

Chemical gettering of the deposit on the microbalance pan was not observed for any of the elements on which absolute f-value measurements were made. Gettering would

appear as an increase in pan weight with the shutter closed, which could not be reversed by heating of the pan.

When the supply of metal in the crucible was running out, the deposit rate at constant crucible temperature was observed to fall off gradually. A formula to correct the observed deposit rate for the effect of decreasing impulse will now be derived.

Let  $W_0$  be the weight of the pan before the shutter is opened. At the time  $t_1$  the shutter is opened and mass is allowed to deposit on the pan until a time  $t_2$  when the shutter is closed. The following equations can be written for the apparent weight of the pan at the two times  $t_1$  and  $t_2$ :  $W_1 = W_0 - F_1$  and  $W_2 = W_0 - F_2 + \int_{t_1}^{t_2} G(\tau) d\tau$ . The observed deposit rate,  $G_{obs}$ , is then  $(W_2 - W_1)/(t_1 - t_2)$ . Using the impulse measurements this expression can be corrected to give  $G_{cor} = G_{obs} - (F_1 - F_2)/(t_1 - t_2)$ .

F. The Photomultiplier Detector

Bell (17) states that the photographic process is useful for the study of absorption lines with equivalent widths greater than  $2 \text{ m}\text{\AA}$ . Work was undertaken to design a photomultiplier detector which could be used for lines as small as  $.4 \text{ m}\text{\AA}$  in equivalent width.

The grating used for this work was mounted in a 21 ft. 10 in. Rowland spectrograph and had a ruled area 12 cm. by 5 cm. with 600 rulings per mm. Using a narrow line emission source, the entrance slit of the spectrograph was closed until maximum sharpness of the image was obtained, and further narrowing of the slit merely decreased the output light intensity. This entrance slit width, at which maximum resolution was obtained, was found to be 30 microns. The dispersion of the spectrograph was  $1.25 \text{ m}\text{\AA}/\text{micron}$  in the second order. The magnification at  $3000 \text{ \AA}$  of the image of the entrance slit was 1.06. Thus monochromatic light at  $3000 \text{ \AA}$  should appear to have a spread of at least  $50 \text{ m}\text{\AA}$  at the image plane of the grating. In practice, when doppler broadened absorption lines with full widths at half maximum of  $8 \text{ m}\text{\AA}$  were imaged by the spectrograph, they were spread over a region of at least  $100 \text{ m}\text{\AA}$ .

This smearing of the doppler profiles of the absorption lines by the spectrograph meant that the change in continuum intensity because of the presence of an absorption

line of  $.4 \text{ mA}^\circ$  equivalent width would be less than 1%, even at the center of the line. If this 1% change in continuum intensity were detected by a photomultiplier whose output, when displayed on a meter or chart recorder, was adjusted to read continuum intensity as full scale, it would be impossible to measure the 1% change to an accuracy of 5%. With a continuum whose intensity was constant to .01%, this problem could be solved by subtracting a constant reference voltage from the continuum signal and displaying the difference voltage as full scale on a chart recorder. Using a difference signal equal to 5% of the continuum signal, the changes in continuum because of a 1% absorption line could then be measured to an accuracy of 5%. Unfortunately, the high pressure mercury discharge lamp used as a continuum source for this experiment was not stable as a function of time. Rapid variation in continuum intensity, of at least 1%, were very common. Also, the lamp output intensity decreased slowly as a function of time because of deposition of cooling water salts on the quartz water jacket.

Therefore, it was decided to use the intensity of a portion of the continuum  $6\text{A}^\circ$  away from the absorption line as a reference signal with which to perform the subtraction described above. Noise due to fluctuations in lamp intensity would be common to the two signals and thus nearly eliminated when they were subtracted. Details of the design of the photomultiplier detector are given in

G. M. Lawrence's thesis (21). A subtraction which allowed 10% of the continuum signal to be displayed full scale on a strip chart recorder was used for most the work reported here.

One technique of equivalent width measurement which was considered employed a stationary slit, wide enough to cover the whole wavelength interval into which the spectrograph spread an absorption line. A shutter in the vacuum chamber, just above the crucible orifice, was used to block the atomic beam. Measurement of the difference in light intensity, coming through the wide slit, with the atomic beam shutter open and closed allowed calculation of the equivalent width of the line, provided the width of the slit was known.

Difficulties in positioning the slit accurately and lack of knowledge of the exact width of the spectral region over which the absorption line was spread by the spectrograph meant that a minimum slit width of  $160 \text{ mA}^\circ$  was necessary. However, the change in signal from this wide slit would be only .25% because of the presence of a line of equivalent width  $.4 \text{ mA}^\circ$ . The noise limitations in the photomultiplier detector were such, that even using the subtraction technique, this small change in signal could not be measured to the desired accuracy of 10%.

The technique which was adopted involved the use of a narrow exit slit with a width of 15 microns. This slit was moved at a constant velocity back and forth across the

absorption line. Details of the design of the constant velocity driving mechanism are given by G. M. Lawrence (21). The use of this narrow exit slit resulted in at least a factor of two increase in the variation of the continuum signal at the peak of a line as compared with the variation when a wide slit was used. The scanning speed used was .0025 in./min. (79.5 mA<sup>0</sup>/min. in second order). Various checks made on the constancy of this speed indicated that it was always within less than 5% of the nominal value.

Because the two slits of the photomultiplier were separated by only 6 A<sup>0</sup>, it was possible to study absorption lines which were on the wings of the pressure broadened mercury emission lines where the continuum intensity was varying rapidly as a function of wavelength. In this case the photomultiplier has a definite advantage over photographic plates because accurate calibration of plates is very difficult if the continuum is varying rapidly.

Equivalent widths were obtained from the output tracings of the photomultiplier by drawing in a base line representing the continuum signal in the absence of absorption and then measuring the area under the line profile thus determined. With the constant velocity scanner method, equivalent widths as small as .4 mA<sup>0</sup> were measured with a standard deviation of about 15%.

Figure III shows an actual tracing of the indium I resonance line  $\lambda_{4101.76}$ . The hyperfine structure components,

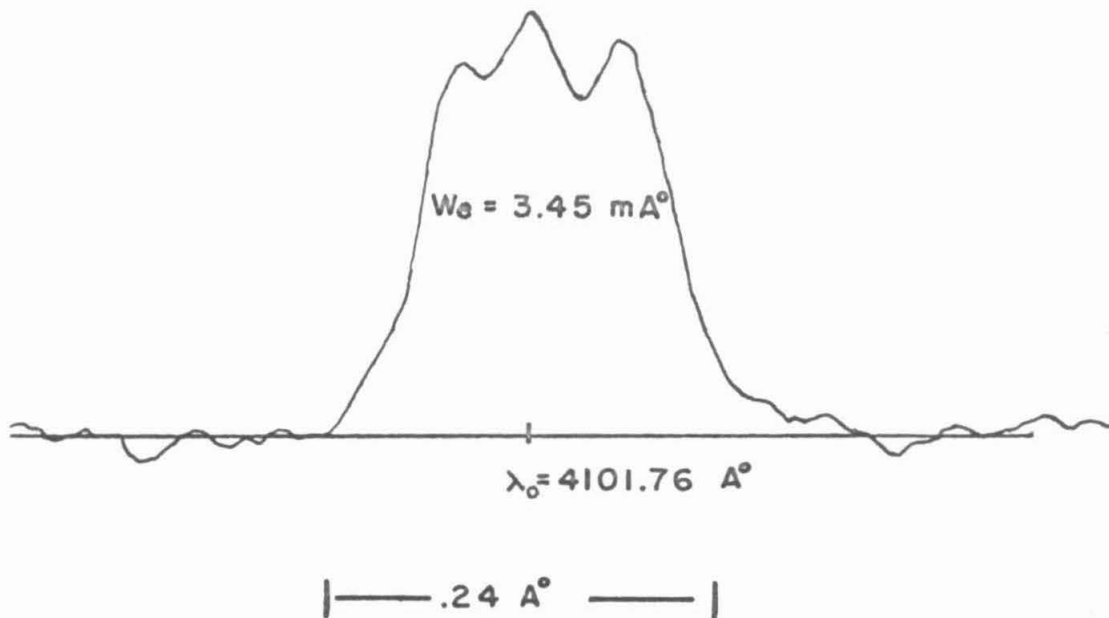
which are separated by about  $50 \text{ m}\text{\AA}$ , are partially resolved.

Figure IV shows two tracings of an absorption line too weak to enable its equivalent width to be measured accurately. This line is so small that its profile is easily altered by the background noise in the detector.

# FIGURE III

Hyperfine Structure for the  
 $\lambda 4101.76$  Line of Indium I

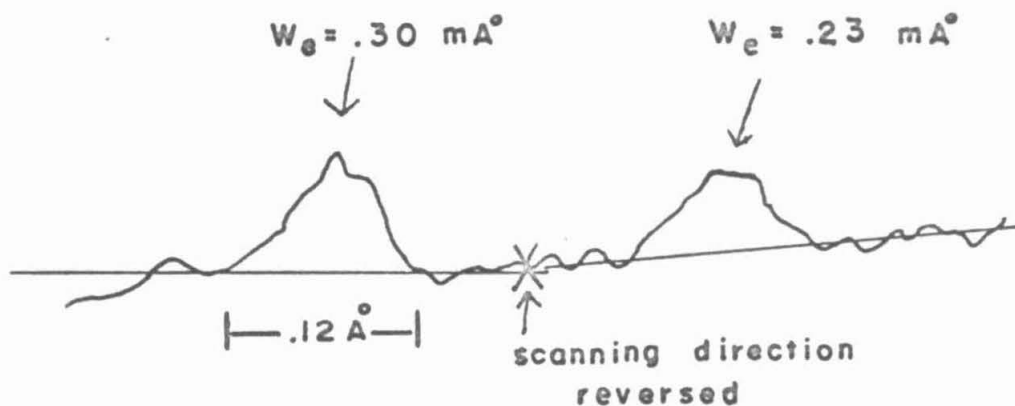
$F_{\text{initial}}$	$F_{\text{final}}$	Splitting	Relative Intensity
5	4	$\lambda_0 - 56.5 \text{ m}\text{\AA}^\circ$	33
5	5	$\lambda_0 + 7.6 \text{ m}\text{\AA}^\circ$	22
4	5	$\lambda_0 + 5.5 \text{ m}\text{\AA}^\circ$	33
4	4	$\lambda_0 - 9.3 \text{ m}\text{\AA}^\circ$	12



# FIGURE IV

## Photomultiplier Scanner

## Output Tracings



### G. Temperature Measurements

Crucible temperatures for all elements except thallium were measured by looking into the orifice of the crucible with an optical pyrometer. Corrections were made for the absorption of radiation by the windows through which the orifice was viewed. These corrections are discussed in detail in Bell's thesis (17).

The platinum to platinum 10% rhodium thermocouple used to measure temperatures for thallium was checked against the optical pyrometer at temperatures between 900 and 1150 °C. They were found to agree to within about 10 °C throughout this temperature range. As will be shown in the next section, the experimentally determined f-values depended only on the square root of the absolute temperature for lines arising from the ground state. An error of 10 °K will therefore not appreciably effect the calculated f-value except for lines from levels more than .2 ev. above the ground state.

## H. Discussion of Errors

All experimental results, reported in the following tables, have been listed with their standard deviations from the mean. The standard deviations range from a low of about 5% to a high of 13%. If the errors were purely random, the standard deviations could each be divided by the factor  $\sqrt{n-1}$ , where n would be the total number of determinations made of the f-value in question, to get an estimate of the error in the mean. Because of undetermined systematic errors, however, this procedure would be of little value.

The following formula was used in calculation of f-values from experimentally determined quantities:  $f = QCT/G'$ . For  $W_e/\Delta\lambda'_0 < .4$ , that is, on the linear part of the curve of growth, this becomes:

$$f = \text{constant} \left\{ \frac{W_e Q \sqrt{T}}{S_{in} \gamma \cdot G \cdot B.F.} \right\} \cdot$$

Estimates of the systematic errors in the above quantities will now be given.

$W_e$ : The electronic circuits involved in translating photomultiplier current into a tracing on the chart recorder were accurate to 1%. The calibration of the planimeter used to measure areas under line profiles was accurate to .3%. The speed with which the line was scanned was perhaps the major source of error. Attempts to measure it accurately failed because of lack of a velocity transducer

which could measure a speed of .0025 in./min. with an accuracy of 1%. A reasonable estimate of the scanning speed error would be 4% for a given setting of the scanner. This systematic error would probably have varied for different positions of the drive screw and spectrometer camera.

G: The electronics of the automatic microbalance and the strip chart recorder were accurate to at least 1%. The vacuum calibration of the balance, using standard .1% 1 mgm. riders, was accurate to .5%. Errors in determining the deposit rates from the output tracings were all random.

T: A conservative estimate of the error in temperature would be 20 °K. At 1000 °K this would be an error of 1% in the square root of T.

Q: The light beam was typically 1.6 in. above the crucible orifice. Errors in measuring the geometrical quantities in Q were small. Errors in Q were thus less than .5%.

$\sin\gamma$ :  $\gamma$  was kept as large as possible to make the effective doppler width of the atomic beam as large as possible. The distances to be measured in determining  $\gamma$  were less than .5 in. Lack of knowledge of the exact location of the effective crucible orifice effected the accuracy of the determination of  $\sin\gamma$ . Errors introduced by  $\sin\gamma$  were less than 1%.

B.F.: For lines from levels more than .2 ev. above the ground state, an error of 20 °K could produce an error

of about 3% in the determination of the population of the excited state.

The effect of the light beam being a thin sheet instead of a pencil of rays was examined theoretically. With the light beam passing 1.6 in. above the crucible orifice the error from this source would not be more than .3% for a total light beam width of .25 in.

The effect of an appreciable amount of scattered light would be to shift the experimental curve of growth and, therefore, make it impossible to fit with a single parameter. The curve of growth shown in figure V indicates a very good fit with one parameter. This, in turn, indicates the presence of negligible scattered light.

The comparison of measured impulse forces with those calculated from the atomic beam theory showed agreement to within about 1%. The systematic errors, because of the combined effects of atoms bouncing off the pan and deviations in the velocity distribution of the atomic beam caused by collisions at the crucible orifice, are estimated to be not more than 2%.

If all the systematic sources of error combined in the worst possible way, the above estimates lead to a maximum systematic error of 13% for lines arising from levels within .15 ev. of the ground state, and about 16% for lines arising from higher excited states.

#### IV. EXPERIMENTAL RESULTS

In the following six sections the experimental results of the work on 25 lines of six elements will be presented. The particular features of each element which are relevant to the measurement of its absolute f-values with the atomic beam apparatus are discussed.

Tables I through VI contain the important experimental quantities which entered into the calculation of absolute f-values. The wavelength of the transition and the mean of the measured f-values are given for each line. The uncertainty listed is the standard deviation of the experimental sample. The first column in each table gives the crucible temperature in  $^{\circ}\text{K}$ , and the second column gives the calculated Boltzmann factor for that temperature. The data were taken by keeping the crucible at a constant temperature and scanning back and forth across the line, reading the deposit rate each time the scanner passed over the line. The third column gives the minimum and maximum Boltzmann factor corrected deposit rates observed at the single crucible temperature. In the fourth column the minimum and maximum equivalent widths are tabulated. The fifth column lists the atomic beam doppler width calculated at the temperature given in the first column. The sixth column gives  $Q$  in the appropriate units to allow calculation of the f-value using equation 8. The seventh column indicates the number of scans made, and the final one contains the mean f-value obtained for that series of scans.

A. Chromium I

The astrophysical importance of chromium has motivated a considerable amount of past work in this laboratory on the absolute f-values of the six strong absorption lines from the ground state. It was felt that further work on chromium was necessary because of the disagreements and inconsistencies in the results of previous investigations.

Chromium presented no difficult experimental problems. No hyperfine structure of the ground state has been observed (23). The ground term of chromium,  $a^7S_3$ , is single, and there are no other low lying terms; therefore, 100% of the atoms are in the ground state at temperatures reached during this experiment.

Chromium has an unusually high vapour pressure while still in the solid state. In fact, all the runs made on chromium were made below the melting temperature. Since it was observed that elements with a tendency to sublime will sputter if heated in the powder form, only lumps of 99.5% pure chromium were used. Zirconia crucibles were used on all chromium runs and appeared to undergo no chemical reaction with the hot chromium. Chromium vapour tended to condense on the cooler parts of the zirconia crucibles, which unfortunately were around the orifice. This deposition produced a tunnel leading from the interior of the crucible to the orifice. For the highest deposit rates, where the pressure of chromium vapour inside the

crucible rose to above .2 Torr, this tunnel may have effected the velocity distribution of the outgoing beam. Most of the work done on chromium was carried out at low atomic beam densities to keep the mean free path of the atoms in the crucible long, compared to the orifice dimensions.

Figure V is the curve of growth obtained for the chromium line  $\lambda 3579$ . The dots represent experimental values of  $W_e/\Delta\lambda'_D$  plotted on a log-log scale against experimental values of  $G'/QT$  ( $G'$  is equal to  $G$  for chromium).  $G'/QT$  is proportional to  $NL/\sqrt{T}$  for the atomic beam.

The curve of growth for the atomic beam gives a relationship between  $W_e/\Delta\lambda'_D$  and  $C$ ; but by equation 4,  $C = fG'/QT$ . An important test of the theoretical curve of growth relation,  $W_e/\Delta\lambda'_D = H(C)$ , can thus be made by comparing  $\log(H^{-1}(W_e/\Delta\lambda'_D))$  with  $\log(G'/QT)$  over a wide range of  $W_e/\Delta\lambda'_D$ . It is necessary to attain values of  $W_e/\Delta\lambda'_D$  greater than 1, so that the curve of growth relation will be nonlinear. If  $\log(H^{-1}(W_e/\Delta\lambda'_D))$  and  $\log(G'/QT)$  differ by only a constant over this wide range it can be concluded that the theory agrees with the experimental results.

The theoretical curve in figure V was obtained by plotting  $\log(W_e/\Delta\lambda'_D)$  against  $\log(C/f)$ . The  $f$ -value chosen was the mean of the experimental values. It is clear that a horizontal shift of  $-\log(f)$  was all that was needed to fit the experimental points with the theoretical curve of growth.

Figure VI is a graph of impulse forces against deposit rates taken from the data used to plot the curve of growth shown in figure V. These data are of particular interest because the deposit rates vary over nearly a factor of 40. The dots are experimental points. Each cluster of points corresponds to a fixed crucible temperature. These temperatures are indicated on the graph. The solid curve is a graph of the relation  $F = 17.5\sqrt{T/M} \cdot G$  which was calculated by assuming that the atomic beam was formed by effusive flow and that all the atoms impinging on the pan stick. It is interesting that the experimental points for the very highest temperature lie along the theoretical curve even though the mean free paths of the chromium atoms in the crucible were about the size of the orifice (see part III section A). The agreement between theory and experiment shown in figure VI was taken as an indication that less than 1% of the chromium atoms were bouncing free of the pan.

The microbalance tracings made during the series of scans of the line  $\lambda 3579$  showed definite evidence of gas absorption during the first two minutes after the shutter was closed. This was particularly evident when the microbalance output was on the most sensitive scale, displaying 0 to 25  $\mu\text{gm}$ . full scale on the chart recorder. The gas absorption rates observed were roughly .01  $\mu\text{gm}/\text{sec}$ .

From table I it can be seen that the average f-value for  $\lambda 3579$  obtained at the lowest crucible temperature is about 5% lower than the grand average. At this lowest

FIGURE V CURVE OF GROWTH

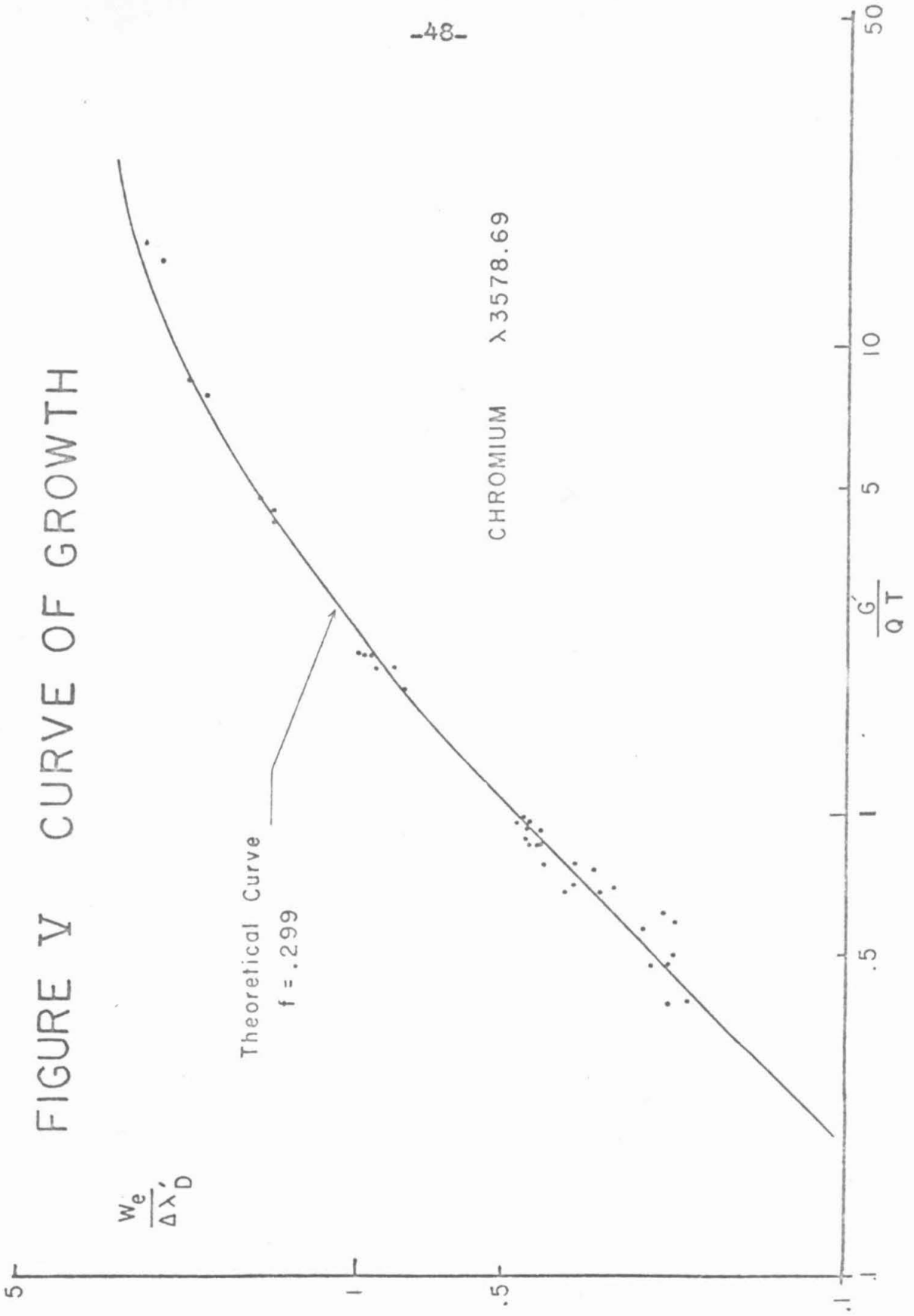
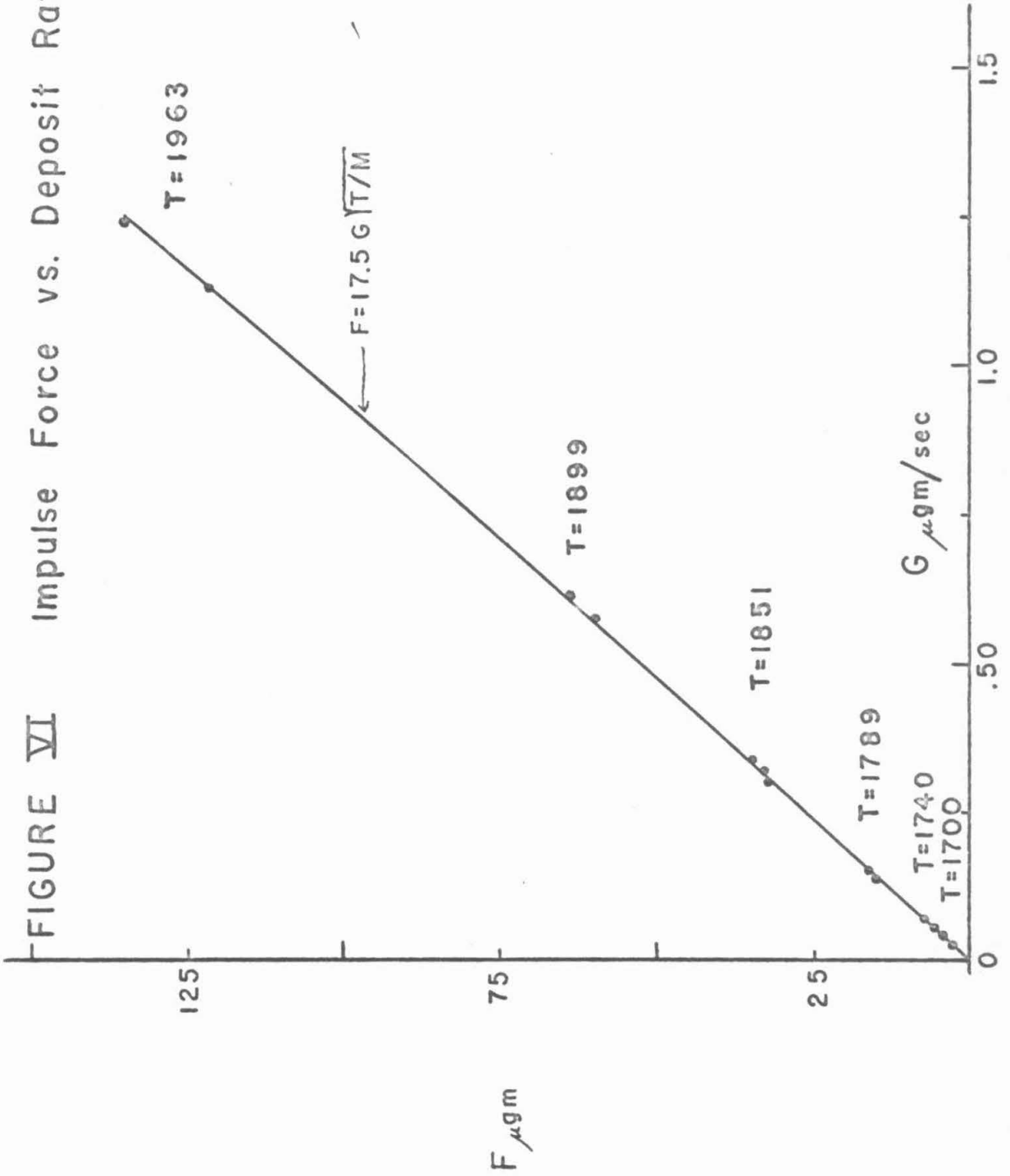


FIGURE VI Impulse Force vs. Deposit Rate



temperature the deposit rate was roughly  $.03 \mu\text{gm./sec.}$ , which is only 3 times the gas absorption rate observed after the shutter was closed. This implies that the rate of gas absorption occurring during the actual deposition of chromium was not more than  $.002 \mu\text{gm./sec.}$ , because a higher rate would have increased the observed deposit rate and would have thereby caused the calculated f-value to be more than 5% too low.

Comparison of impulse forces received by the balance pan when the shutter was opened with those received when the shutter was closed indicated that roughly the same amount of gas was being driven off the pan upon exposure to the atomic beam as was absorbed in the period after the shutter was closed. These observations support the hypothesis that a thin film of gas weighing a few  $\mu\text{gm.}$  forms on the freshly deposited metal only after the stream of high temperature atoms and radiation from the furnace stops, and that this gas is driven off again once the atomic beam deposition is resumed.

Table I. Chromium I Data

T °K	B.F.	G' range Å <sup>2</sup> /sec	W <sub>e</sub> range mÅ <sup>2</sup>	$\Delta\lambda_0'$ mÅ <sup>2</sup>	$Q_{+3}$ x10 <sup>+3</sup>	# of scans	f
<u><math>\lambda = 3578.69</math></u>							
1714	1.0	.04-.05	1.7-2.2	5.75	.039	6	.293
1744	1.0	.06-.07	2.4-2.7	5.80	.039	6	.301
1733	1.0	.05-.06	2.4-2.6	5.78	.039	6	.318
1789	1.0	.14-.15	5.4-5.8	5.87	.039	6	.316
1859	1.0	.30-.34	8.9-9.5	5.98	.039	3	.293
1899	1.0	.57-.61	13.-14.	6.04	.039	2	.298
1963	1.0	1.1-1.2	16.-17.	6.15	.039	2	.257
1695	1.0	.03-.04	1.2-1.5	5.70	.039	8	.288
<u>f = .297 ± .026</u>							
<u><math>\lambda = 3593.49</math></u>							
1793	1.0	.10-.11	3.2-3.8	5.89	.0388	6	.247
1738	1.0	.04-.06	1.4-1.5	5.80	.0388	4	.228
<u>f = .239 ± .017</u>							
<u><math>\lambda = 3605.33</math></u>							
1842	1.0	.14-.15	3.3-3.7	6.00	.0387	8	.188
1745	1.0	.05-.06	1.1-1.3	5.84	.0387	8	.164
1882	1.0	.31-.33	6.6-7.1	6.06	.0387	4	.191
<u>f = .179 ± .017</u>							

Table I. (Cont.)

T °K	B.F.	G' range $\mu\text{gm}/\text{sec}$	$W_e$ range $\text{mA}^\circ$	$\Delta\lambda_0'$ $\text{mA}^\circ$	$Q$ $\times 10^3$	# of scans	f
<u><math>\lambda = 4254.35</math></u>							
1831	1.0	.26-.30	3.5-4.0	7.32	.0324	4	.0726
1740	1.0	.09-.10	1.2-1.5	7.04	.0324	4	.0682
1916	1.0	.30-.30	3.1-5.1	7.48	.0324	10	.0886
1808	1.0	.14-.15	.21-.25	7.13	.0330	6	.0805
1844	1.0	.21-.26	3.2-3.8	7.20	.0330	5	.0807
1904	1.0	.41-.45	5.9-6.5	7.32	.0330	4	.0861
1996	1.0	1.0-1.2	11.-13.	7.50	.0330	4	.0783
1827	1.0	.09-.14	1.6-2.4	7.15	.0319	8	.0818
1879	1.0	.22-.26	3.5-4.4	7.25	.0319	4	.0791
<u><math>\bar{f} = .0805 \pm .0071</math></u>							
<u><math>\lambda = 4274.80</math></u>							
1811	1.0	.16-.20	2.0-2.4	7.05	.0324	6	.0575
1846	1.0	.24-.27	2.7-3.2	7.12	.0324	4	.0611
1863	1.0	.19-.22	2.5-2.8	7.20	.0321	6	.0636
<u><math>\bar{f} = .0619 \pm .0030</math></u>							
<u><math>\lambda = 4289.72</math></u>							
1842	1.0	.19-.23	1.6-2.2	7.16	.0327	6	.0463
1920	1.0	.35-.62	5.1-3.4	7.31	.0327	17	.0477
1841	1.0	.08-.14	.76-1.4	7.13	.0322	5	.0478
1928	1.0	.45-.55	3.8-4.3	7.30	.0322	3	.0447
<u><math>\bar{f} = .0470 \pm .0029</math></u>							

## B. Gallium I

Gallium forms a useful atomic beam from a graphite crucible at temperatures above 1140 °C. Examination of impulse forces detected by the microbalance upon closing the shutter indicated that at least 99% of the gallium atoms were sticking to the conical pan.

The only low lying term in the gallium Grotrian diagram is  $4s^2 4p^2 P^o$ , The  $J = 3/2$  level is .1024 ev. above the  $J = 1/2$  level. At the temperatures used for this experiment both levels were about equally populated.

Gallium is composed of two isotopes,  $A = 71$  (40%) and  $A = 69$  (60%). Both isotopes have a nuclear spin of  $3/2$ . Of the five lines studied, only two  $\lambda_{2874}$  and  $\lambda_{2943.6}$ , were measured with equivalent widths large enough that  $W_e/\Delta\lambda_p$  was greater than .4. The other three lines were kept on the linear part of the curve of growth for all scans.

For  $\lambda_{2874}$ , each isotope has two hyperfine structure components, and the patterns for the two isotopes are separated from each other by about  $1 \text{ mÅ}^o$  (23). The effective doppler width for the atomic beam was about  $4.2 \text{ mÅ}^o$ . Thus, the isotopic components were blended in a complicated way. The nuclear magnetic dipole interaction produced two components for each isotope which were not blended because of doppler broadening. The intensity ratio of the components for a single isotope was 5 : 3. For all scans

of  $\lambda_{2874}$ ,  $w_e/\Delta\lambda_D$  was kept below .8, and C was split 5:3 to give the curve of growth for the composite line. For these moderately weak lines, each of the two hyperfine components were nearly on the linear part of the curve of growth, and it was felt that little error would result from neglecting the isotopic splitting.

For  $\lambda_{2943.6}$ , each isotope has 4 hyperfine structure components, and the patterns of the two isotopes are separated by about .3 mÅ<sup>0</sup>. Since the single isotope splitting was less than the atomic beam doppler width, the various components were blended together. As a first approximation to an exact treatment of the splitting, C was divided into two equal parts in computing the curve of growth for the blended line.

Because of the blending of the components of  $\lambda_{2943.6}$ , it would have been best to have scanned only weak lines on the linear part of the curve of growth. This was not done because the proximity in wavelength of  $\lambda_{2943.6}$  and  $\lambda_{2944.18}$  made it possible to scan the two lines consecutively at a single crucible temperature. As the f-value of  $\lambda_{2944.18}$  is smaller than the f-value for  $\lambda_{2943.6}$  by a factor of nine, the equivalent width for  $\lambda_{2943.6}$  had to be larger than 3.5 mÅ<sup>0</sup> so that the equivalent width for  $\lambda_{2944.18}$  would be large enough to measure with reasonable accuracy.

Table II. Gallium I Data

T °K	B.F.	G' range $\mu\text{gm}/\text{sec}$	$W_e$ range $\text{mA}^\circ$	$\Delta\lambda'_p$ $\text{mA}^\circ$	Q $\times 10^{+4}$	# of scans	f
<u><math>\lambda = 2874.24</math></u>							
1503	.524	.07-.08	2.6-3.2	4.29	.283	6	.237
1490	.527	.05-.06	1.9-2.3	4.27	.283	6	.221
1440	.533	.02-.03	.91-1.1	4.20	.283	6	.238
1547	.519	.09-.12	2.9-3.7	4.35	.268	6	.203
1484	.528	.05-.05	1.7-1.9	4.26	.268	3	.214
1406	.538	.02-.02	.54-.58	4.15	.268	7	.217
1498	.526	.06-.07	2.1-2.4	4.30	.283	4	.248
<u><math>\bar{f} = .225 \pm .019</math></u>							
<u><math>\lambda = 2944.175</math></u>							
1605	.490	.24-.30	.85-1.3	4.55	.276	5	.0229
1545	.482	.11-.17	.37-.49	4.46	.268	5	.0206
<u><math>\bar{f} = .0218 \pm .0026</math></u>							
<u><math>\lambda = 2943.6</math></u>							
1605	.490	.21-.25	6.4-7.5	4.55	.276	4	.183
1545	.482	.11-.17	3.2-4.5	4.46	.268	5	.188
<u><math>\bar{f} = .186 \pm .019</math></u>							

Table II. (Cont.)

T °K	B.F.	G' range μgm/sec	W <sub>e</sub> range mA°	$\Delta\lambda_p'$ mA°	Q x10 <sup>+4</sup>	# of scans	f
<u><math>\lambda = 4032.98</math></u>							
1363	.544	.06-.08	1.0-1.3	5.63	.337	9	.0757
1383	.541	.07-.10	1.1-1.6	5.67	.337	12	.0739
1407	.538	.13-.15	1.8-2.1	5.72	.337	9	.0659
1385	.541	.09-.09	1.2-1.6	5.68	.337	10	.0735
1398	.539	.11-.14	1.4-1.9	5.70	.337	6	.0648
<u><math>\bar{f} = .0719 \pm .0072</math></u>							

<u><math>\lambda = 4172.06</math></u>							
1408	.462	.10-.11	1.7-2.1	5.93	.326	8	.0762
1358	.454	.04-.05	.74-1.1	5.82	.326	8	.0801
1389	.459	.08-.09	1.3-1.5	5.89	.326	9	.0736
<u><math>\bar{f} = .0764 \pm .0117</math></u>							

### C. Indium I

Indium forms an atomic beam at temperatures above 960 °C, which is dense enough to allow observation of the strong lines from the ground term. Indium was vapourized from a graphite crucible.

The microbalance tracings made during the deposition of indium were quite linear and showed no signs of gettering or serious gas absorption on the conical pan. Comparisons of experimental impulse forces with those calculated from the observed deposit rates indicated that less than 1% of the indium atoms were bouncing free of the pan. Several deposit tracings were taken with a flat pan. Examination of the impulse forces showed that they were about 10% larger than calculated, which indicated that some of the atoms were bouncing off the flat pan. This observation supported the theory that the conical pans had a high collection efficiency because the atoms had to bounce off the pan surface several times before actually escaping.

The ground term of indium is  $5s^25p^2P^0$ . The  $J = 3/2$  level lies .274 ev. above the ground level  $J = 1/2$ . There are no other low lying terms. At the temperatures attained in the crucible, approximately 15% of the indium atoms were in the  $J = 3/2$  state. The population of the  $J = 3/2$  state was a rather strong function of temperature, changing by 8% in 50 °C.

Indium has a nuclear spin of  $9/2$  and therefore consider-

able hyperfine splitting is observed for the lines whose  $f$ -values were measured. Because of the large nuclear spin the theoretical intensity ratios were calculated from the general formulae given by Kuhn (26). Of the five lines studied only two,  $\lambda 4101$  and  $\lambda 3039$ , were observed with large enough equivalent widths to be on the non-linear part of the curve of growth. For both lines, the component separations were greater than the atomic beam doppler widths (23). Figure III shows an actual tracing of the  $\lambda 4101$  line. For  $\lambda 4101$  the relative strengths of the  $C_1$  were .33 : .22 : .33 : .12. For the line  $\lambda 3039$ , they were .55 : .45.

Table III. Indium I Data

T °K	B.F.	G' range μgm/sec	W <sub>e</sub> range mA°	Δλ' <sub>g</sub> mA°	Q x10 <sup>+4</sup>	# of scans	f
<u>λ = 3039.4</u>							
1311	.850	.07-.08	2.7-3.2	3.12	.268	6	.306
1261	.861	.03-.03	1.3-1.5	3.06	.268	6	.287
1301	.852	.07-.07	2.2-2.7	3.12	.268	3	.256
1337	.843	.12-.13	3.9-4.4	3.15	.268	5	.261
1276	.857	.04-.05	1.6-1.8	3.08	.268	4	.256
1349	.841	.11-.14	5.1-5.5	3.15	.268	5	.312
1384	.833	.23-.24	6.8-7.8	3.20	.268	2	.284
1346	.842	.09-.12	3.3-4.6	3.31	.289	10	.267
1416	.825	.31-.36	8.6-10.	3.40	.289	7	.268
1455	.816	.57-.60	12.-13.	3.44	.289	4	.267
1294	.853	.04-.05	1.6-2.1	3.25	.289	5	.274
1255	.863	.02-.03	.95-1.2	3.20	.289	5	.282

$$\bar{f} = .277 \pm .023$$

$$\lambda = 3256.09$$

1328	.156	.04-.04	.97-1.1	3.54	.418	3	.233
1346	.164	.06-.06	1.5-1.7	3.56	.418	5	.236
1249	.137	.02-.02	1.1-1.5	3.37	.182	4	.237
1220	.130	.01-.01	.74-.81	3.33	.182	4	.232

$$\bar{f} = .235 \pm .021$$

Table III. (Cont.)

T °K	B.F.	G range $\mu\text{gm/sec}$	$W_e$ range $\text{mA}^0$	$\Delta\lambda_0$ $\text{mA}$	$Q$ $\times 10^4$	# of scans	f
<u><math>\lambda = 3258.56</math></u>							
1413	.180	.19-.23	.44-.65	3.65	.418	12	.0266
1341	.157	.12-.17	.73-1.0	3.49	.182	8	.0253
1321	.153	.10-.10	.53-.66	3.47	.182	2	.0224
<u><math>\bar{f} = .0258 \pm .0032</math></u>							
<u><math>\lambda = 4101.76</math></u>							
1297	.849	.13-.16	2.2-3.5	4.40	.333	2	.110
1279	.853	.09-.12	1.9-2.4	4.37	.333	6	.124
1351	.835	.40-.51	5.6-8.6	4.49	.333	8	.115
1333	.842	.18-.22	4.0-4.5	4.46	.333	6	.125
<u><math>\bar{f} = .120 \pm .011</math></u>							
<u><math>\lambda = 4511.31</math></u>							
1366	.169	.09-.09	1.9-2.1	5.01	.302	6	.108
1336	.161	.05-.07	1.3-1.7	4.95	.302	6	.114
<u><math>\bar{f} = .111 \pm .009</math></u>							

D. Tin I

Tin forms an atomic beam of sufficient density so that its absorption lines may be observed at temperatures above 1450 °C. Tin can be vapourized in graphite crucibles. The microbalance tracings made during the deposition of tin were very linear and steady, and they indicated no gettering or absorption of gas. Comparison of theoretical and experimental impulse forces showed that less than 1% of the tin atoms were bouncing free of the pan.

Tin has ten isotopes, three of which have non-zero nuclear spin and thus appreciable hyperfine splitting of low lying terms. These three isotopes comprise only 16% of naturally occurring tin. For five of the six tin lines studied, the equivalent widths were kept small enough that the lines were on the linear part of the curve of growth. For the strongest line,  $\lambda 2863.32$ , for which some large equivalent widths were observed, C was split in the ratio .84 : .05 : .11.

All of the lines in the multiplet  $5p^2 \ ^3P - 5p^2 \ ^3P^0$  were measured. This was possible because the energy splitting of the lower term,  $5p^2 \ ^3P$ , was small enough that even the  $J = 2$  level was populated with about 15% of the atoms at the temperatures attained in the crucible. The  $J = 1$  level was .21 ev. and the  $J = 2$  level .425 ev. above the ground state.

Table IV. Tin I Data

T °K	B.F.	G' range μgm/sec	W <sub>e</sub> range mA°	$\Delta \lambda'_0$ mA°	Q x10 <sup>+4</sup>	# of scans	f
<u><math>\lambda = 2863.32</math></u>							
1751	.488	.11-.12	1.6-1.9	3.49	.490	5	.237
1780	.481	.16-.17	2.1-2.4	3.52	.490	6	.220
1814	.474	.19-.22	2.0-2.5	3.56	.490	6	.173
1866	.456	.29-.29	3.1-3.5	3.60	.490	6	.188
1972	.437	.68-.85	0.2-6.7	3.70	.490	6	.174
1724	.495	.05-.06	.50-.90	3.47	.490	8	.187
1818	.471	.27-.35	3.0-3.9	3.55	.490	10	.185
1846	.466	.33-.35	3.6-3.8	3.59	.482	3	.183
1786	.486	.19-.20	2.2-2.6	3.53	.482	7	.194

$$\bar{f} = .192 \pm .021$$

$$\lambda = 3034.12$$

1839	.374	.29-.32	1.4-1.6	3.79	.455	6	.0685
------	------	---------	---------	------	------	---	-------

$$\bar{f} = .0685 \pm .0040$$

$$\lambda = 2706.51$$

1914	.379	2.6-3.3	.50-.64	3.45	.509	6	.084
------	------	---------	---------	------	------	---	------

$$\bar{f} = .084 \pm .009$$

Table IV. (Cont.)

T. °K	B.F.	G range $\mu\text{gm}/\text{sec}$	$W_e$ range $\text{mA}^\circ$	$\Delta\lambda_D$ $\text{mA}^\circ$	$Q_{+4}$ $\times 10^{+4}$	# of scans	$\bar{f}$
<u><math>\lambda = 3009.14</math></u>							
1899	.378	.80-.84	1.6-1.8	3.82	.459	4	.0279
1836	.374	.38-.45	.81-1.2	3.75	.459	5	.0320
1691	.360	.33-.38	2.0-2.2	3.54	.193	4	.0353
1658	.356	.19-.21	1.1-1.5	3.50	.193	4	.0355
<u><math>\bar{f} = .0326 \pm .0041</math></u>							
<u><math>\lambda = 3175.05</math></u>							
1869	.163	.18-.20	.97-.98	4.00	.435	2	.0622
1949	.177	.16-.35	.80-1.7	4.08	.435	4	.0630
1712	.140	.14-.15	1.7-1.8	3.76	.183	4	.0624
1656	.131	.06-.07	.72-.88	3.69	.183	4	.0610
<u><math>\bar{f} = .0621 \pm .0032</math></u>							
<u><math>\lambda = 2839.99</math></u>							
1823	.156	.11-.11	.88-.91	3.52	.486	3	.121
1881	.166	.12-.27	1.4-1.9	3.58	.486	9	.118
<u><math>\bar{f} = .119 \pm .007</math></u>							

### E. Thallium I

Thallium forms an atomic beam at temperatures below those measurable by the optical pyrometer. A platinum-platinum 10% rhodium thermocouple was used to make all temperature measurements. The thermocouple junction was cemented into one end of the graphite crucible with alundum cement, which served to protect the junction from the molten thallium. The cold junction was at room temperature, and the voltage difference was read on a Wolff potentiometer.

At crucible temperatures of 1000 °K, essentially all of the thallium atoms were in the  $6p\ ^2P_{1/2}$  ground state because the next lowest state,  $^2P_{3/2}$ , lies nearly 1 ev. above the ground state.

Two lines were studied,  $\lambda 3775.72$  and  $\lambda 2767.87$ , both of which have hyperfine structure components separated by more than the doppler width of a single component. The line  $\lambda 3775.72$  has six components, three from the isotope 203 (30%) and three from the isotope 205 (70%) (23). For a single isotope, the three components have the relative intensities 2 : 1 : 1. These combined with the isotopic abundances gives the following splitting for C .35 : .175 : .175 : .15 : .075 : .075. The line  $\lambda 2767.87$  has four hyperfine structure components, two from each isotope. For a single isotope the two components have the intensity ratio 3 : 1; thus C was split .525 : .175 : .225 : .075. The total C for the observed absorption line made up of

unresolved components was then obtained by the method described in part II.

The large standard deviation of the experimental values for the  $f$ -value of the line  $\lambda 2767.87$  was mainly a result of the very small doppler width of  $1.85 \text{ mÅ}^{\circ}$ . With this small doppler width, all the lines scanned were on the non-linear part of the curve of growth, where scatter in  $W_e$  values produces greater scatter in the calculated  $f$ -values.

The microbalance tracings made during the deposition of thallium were quite linear, indicating that the deposit rates were reasonably constant. No evidence of gas absorption was seen.

A graph, like that shown in figure VI, for thallium showed that a third of the impulse forces were about 5% too large. The rest fell nicely along the theoretical curve. It was decided that, averaged over all the data, at least 98% of the thallium atoms were sticking to the pan. This effect may have introduced, at most, a 2% error in the calculated  $f$ -values.

Table V. Thallium I Data

T °K	B.F.	G' range $\mu\text{gm}/\text{sec}$	$W_e$ range $\text{mA}^\circ$	$\Delta\lambda_0'$ $\text{mA}^\circ$	$Q$ $\times 10^{+4}$	# of scans	f
<u><math>\lambda = 3775.72</math></u>							
977	1.0	.31-.35	4.8-5.5	2.59	.362	6	.125
957	1.0	.11-.13	1.9-2.2	2.56	.362	6	.128
977	1.0	.27-.33	4.0-5.3	2.59	.362	10	.127
<u><math>\bar{f} = .127 \pm .008</math></u>							

<u><math>\lambda = 2767.87</math></u>							
956	1.0	.17-.19	2.8-3.4	1.87	.495	9	.292
904	1.0	.48-.66	.99-1.4	1.83	.495	8	.315
917	1.0	.55-.71	1.3-1.5	1.84	.495	6	.307
<u><math>\bar{f} = .304 \pm .038</math></u>							

F. Palladium I

Palladium formed an atomic beam from a graphite crucible at temperatures above 1740 °C. The high temperatures of the furnace caused a considerable amount of outgassing of the inside of the vacuum chamber. Because of this outgassing the pressure in the chamber was about  $7 \times 10^{-6}$  Torr while most of the palladium data was taken.

The evolution of gas from the region of the hot furnace, possibly from the graphite furnace tube itself, generated a wind coming up from the furnace toward the microbalance pan. This wind increased the measured impulse force upon both opening and closing the atomic beam shutter. At the lowest temperature used, the rate of gas evolution decreased and impulse force measurements were obtained which agreed to within 2% with those calculated from the measured deposit rates.

The microbalance pan was observed to absorb several micrograms of gas while the shutter was closed. As in the case of chromium, this gas was driven off within ten seconds after the atomic beam shutter was opened.

Although the impulse force check at the lowest temperature indicated that less than 2% of the atoms were failing to stick to the balance pan, it was felt that the difficulties with wind and gas absorption made the possible error in the measured deposit rates for palladium as high as 5%.

As the lowest term in the palladium Grotrian diagram is  $4d^{10} 1S_0$ , and there are no other low lying terms, all atoms were in the ground state at atomic beam temperatures.

No hyperfine splitting of the ground state of palladium has been observed (23). The line  $\lambda_{2763}$  was the only one studied because the other strong lines from the ground state have wavelengths shorter than  $2500 \text{ \AA}$ .

Table VI. Palladium I Data

T °K	B.F.	G' range μgm/sec	W <sub>e</sub> range mA°	Δλ <sub>0</sub> ' mA°	Q <sub>+</sub> x10 <sup>+4</sup>	# of scans	f
<u>λ = 2763.08</u>							
2105	1.0	.42-.40	.68-.90	3.42	.503	3	.0386
2071	1.0	.25-.72	1.3-.53	3.51	.503	10	.0366
2163	1.0	.56-.88	1.1-1.8	3.67	.503	17	.0359
<u>f̄ = .0361 ± .032</u>							

## V. DISCUSSION

### A. Absolute f-Values

Table VII summarizes the 25 absolute f-values measured in this experiment along with some of the more reliable work by other investigators. The first column lists the six elements studied. The second column contains the wavelengths of the 25 lines and the third column gives the multiplet. The fourth column, under the heading  $f(AB)$ , lists the results of this experiment obtained using an atomic beam apparatus. These f-values may be expected to deviate from the true values by a factor ranging from 1.1 to 1.15 depending on the number of scans made and the degree of error introduced by the Boltzmann factor.

The fifth column, headed  $f(NBS)$ , gives the results obtained by Corliss and Bozman <sup>(3)</sup> derived from arc emission spectra. They quote an expected error of about 85% for their absolute f-values. Some of the difficulties in measuring absolute f-values from arc emission spectra have been discussed in part I.

The sixth column, headed  $f(\text{hook})$ , lists absolute f-values obtained by measuring the anomalous dispersion of the atomic vapour near the absorption line <sup>(11,12,13)</sup>. The change in index of refraction in the vicinity of absorption lines is measured by splitting a beam of light into two parts and letting one pass through the vapour and the other pass through a glass compensating plate so adjusted

that the phase coherence of the two beams is maintained. The relative phase of the two beams varies as a function of wavelength near each absorption line because the index of refraction of the vapour is varying. If the two beams are recombined and sent through a spectrograph, the output of the spectrograph will show alternate dark and bright fringes because of the varying phase difference of the two beams. On either side of an absorption line these fringes have a characteristic hooked appearance. A detailed analysis shows that the square of the separation of the hooks is proportional to  $NfL$  for that line. The vapour column is maintained at thermal equilibrium in a long closed quartz tube. The density of vapour in the column is obtained from vapour pressure data, and thus an absolute  $f$ -value can be calculated. Since the essential quantity involved in determining  $NfL$  is the distance between hooks on a photographic plate, which can be measured with an accuracy of better than 5%, the major source of error in obtaining  $f$  is the vapour pressure data.

The lifetime method, employed to measure the absolute  $f$ -values for gallium and thallium (5), involved the use of a light beam which was modulated at a megacycle frequency. The atomic vapour being studied would absorb light from the sinusoidally modulated incoming beam at the frequencies of its absorption lines. This light was then re-emitted. For a specific transition, the re-emitted light had a shift in phase relative to that of the incoming beam, which was a

simple function of the lifetime of the excited state. By electronically detecting the shift in phase between the incoming and re-emitted light, this lifetime can be measured. Demtroder (5) states that these lifetime measurements were made with an error of less than 3%. The advantage of this method lies in its independence of the actual density of absorbing atoms. Because the lifetime of the excited state is measured, and not the transition probability for a given line, an absolute f-value can be computed directly only if there is a single downward transition out of the excited state. If there are more than one allowed transitions then their relative f-values must be known before the lifetime can be used to give absolute f-values.

The f-values obtained for gallium and thallium by Demtroder are listed in the seventh column. The lifetime measurement in both cases was made on an excited state  $^2S_{1/2}$ . For both elements there are allowed transitions from this state to two lower levels,  $^2P_{1/2}$  and  $^2P_{3/2}$ .

For gallium Demtroder calculated the relative transition probabilities into these two states by using the relative intensities predicted by L-S coupling. These predictions do not agree with the relative f-values obtained by the hook method or by the atomic beam method. Column eight gives corrected f-values for the two gallium lines,  $\lambda 4033$  and  $\lambda 4172$ , calculated using Demtroder's value for the lifetime of the upper state and the relative f-values of the two lines obtained by Ostrovskii and Penkin (13).

In the case of thallium, relative transition probabilities obtained from the work of Vonwiler in 1930 (27) were used by Demtroder to calculate absolute f-values from the measured lifetime. The relative f-values which were thus obtained for the two thallium lines,  $\lambda_{3776}$  and  $\lambda_{5350}$ , do not agree very closely with those obtained by Kvater (28) using the hook method. A corrected f-value for the  $\lambda_{3776}$  line was calculated from Kvater's relative f-values and the lifetime of the upper state. This f-value appears in the eighth column.

The f-values for chromium listed in the seventh column were obtained by Estabrook (10).  $NfL$  was obtained by measuring the equivalent width of absorption lines. The absorbing vapour was confined at thermal equilibrium in a sealed quartz cell and its temperature accurately measured. The vapour pressure data of Speiser, Johnston, and Blackburn (29) was used to obtain absolute f-values.

It is of interest to note that the absolute f-values reported by Ostrovskii (12) (sixth column) are larger by about a factor of two than those reported by Estabrook for the chromium  $a^7S - z^7P^0$  multiplet. Since they both used the vapour pressure data of Speiser et al. the reason for the discrepancy must lie elsewhere. In fact, a log plot of their reported values of  $NfT$  against  $1/T$  clearly shows the factor of two difference. Speiser et al. report a slope of about 20,000 for their vapour pressure curve ( $\log(P)$  against  $1/T$ ). The slope measured from the graph

of  $\log(NfT)$  against  $1/T$  for the data of Estabrook is about 14,000, and for the data of Ostrovskii it is about 8,000. Since the results of Estabrook agree with the atomic beam values, this may indicate that there is some error in the  $Nf$  data obtained with the hook method.

The  $f$ -values listed in the eighth column are reported by Allen (30,31,32). His method was similar to that of Corliss and Bozman in that he used an emission arc source. Published relative  $gf$ -values were used to obtain the arc temperature. Allen gives a factor of two as his probable error. The  $f$ -values listed here are from Allen's latest paper (1960) and have been changed somewhat from the values given in the 1957 paper.

The atomic beam absolute  $f$ -values reported here for the six chromium lines were used to calibrate the relative  $f$ -value scale in the work of Hill (33). The factor  $6 \times 10^{-4}$  will reduce Hill's relative values to an absolute scale.

In their article on the abundances of elements in the solar atmosphere, Goldberg et al. (34) use absolute  $f$ -values in all of their abundance calculations. For the chromium abundance they derive the following formula for the abundance of chromium relative to that of hydrogen:  $\log(N_{Cr}/N_H) + 12 = 1.6 - \log(F_r)$  where  $F_r$  is the factor which is needed to reduce Hill's relative  $f$ -values to an absolute scale. Using the reduction factor given above, the following result is obtained:  $\log(N_{Cr}/N_H) + 12 = 4.82$ .

Goldberg et al. use the f-value of .22 for the indium  $\lambda 4511$  line to obtain the abundance of indium in the solar atmosphere. If the atomic beam value of .11 is used instead, the abundance becomes:  $\log(N_{\text{In}}/N_{\text{H}}) + 12 = 1.45$ .

In the case of gallium, Goldberg et al. list the line  $\lambda 4172$  as the only one that can be used in abundance determination. They use an f-value of .19 obtained from the work of Allen (30) to derive a value for  $\log(N_{\text{Ga}}/N_{\text{H}}) + 12$  of 2.36. If the atomic beam value of .076 is used, the calculated relative abundance of gallium becomes  $\log(N_{\text{Ga}}/N_{\text{H}}) + 12 = 2.76$ .

For tin, the seventh column lists three f-values obtained by N. Moise by using an absorption cell technique (35). Vapour pressure data was used to calculate f after  $N_{\text{fL}}$  was determined from the equivalent widths of lines formed in absorption.

Table VII. Absolute  $f$ -Values

El.	$\lambda$	Multiplet	$f(AB)$	$f(NBS)$ (3)	$f(hook)$	Other Expt. Results
Cr	4254	$a^7S_3-z^7P_4^0$	.081	.077	.15 <sup>(12)</sup>	.084 <sup>(10)</sup> .050 <sup>(32)</sup>
	4275	3- 3	.062	.059	.11	.067
	4290	3- 2	.047	.037	.082	.047
	3579	$a^7S_3-y^7P_4^0$	.30	.23	.49	.084 <sup>(32)</sup>
	3593	3- 3	.24	.20	.39	
	3605	3- 2	.18	.14	.28	
Ga	2874	$4p^2P_{1/2}-4d^2D_{3/2}$	.23	.37	.32 <sup>(13)</sup>	
	2944	3/2- 3/2	.022	.06	.038	
	2943	3/2- 5/2	.19	.38	.29	
	4033	$4p^2P_{1/2}-5s^2S_{1/2}$	.072	.120	.129	.088 <sup>(5)</sup> .084
	4172	3/2- 1/2	.076	.133	.135	.085 .088
In	3039	$5p^2P_{1/2}-5d^2D_{3/2}$	.28	.50	.50 <sup>(13)</sup>	
	3256	3/2- 5/3	.24	.50	.51	
	3259	3/2- 3/2	.026	.12	.079	
	4102	$5p^2P_{1/2}-6s^2S_{1/2}$	.120	.24	.20	
	4511	3/2- 1/2	.111	.17	.22	
Tl	3776	$6p^2P_{1/2}-7s^2S_{1/2}$	.127	.11	.125 <sup>(28)</sup>	.128 <sup>(5)</sup> .122
	2768	$6p^2P_{1/2}-6d^2D_{3/2}$	.30	.24	.272	
Pd	2763	$4d^{10}1s_0-4d^95p^3P_1^0$	.036	.071		

Table VII. (Cont.)

El.	$\lambda$	Multiplet	f(AB)	f(NBS) (3)	f(hook)	Other Expt. Results
Sn	2863	$5p^2 \ ^3P_0 - 6s \ ^3P_1^0$	.192	.65		.332 (35)
	3009	1- 1	.033	.18		.042
	3034	1- 0	.069	.20		
	2706	1- 2	.084	.37		
	3175	2- 1	.063	.098		.065 (35)
	2840	2- 2	.119	.50		

### B. Relative f-Values

Table VIII gives relative f-values within multiplets. The first, second, and third columns list the element, wavelength, and multiplet of the transition. The fourth column gives the theoretical relative f-values for lines within a multiplet. To obtain these, the relative line strengths given by White and Eliason (24) were divided by  $g\lambda$  ( $g$  is  $2J+1$  for the lower state) and then normalized to a scale on which the strongest line in the multiplet had a relative f-value of unity. These relative f-values should be quite accurate for multiplets for which L-S coupling holds, and the spread of wavelengths is not more than  $150 \text{ \AA}$ .

The fifth column lists the relative f-values from this experiment. Since most sources of systematic error would be constant within a multiplet, the relative f-values should be accurate to about 6%.

Relative values from the work of Corliss and Bozman are given in the sixth column. The authors quote an expected error of 30%.

Results obtained using the hook method are given in the seventh column. For the reasons given in the previous section, expected errors are less than 5% for relative f-values obtained with the hook method.

The last column gives the values obtained by Hill (33) for chromium. A King furnace was used to produce a stable

vapour column of sufficient density to allow observation of many of the absorption lines of chromium. As the two multiplets listed here are both spread less than  $40 \text{ \AA}$ , an entire multiplet could be photographed on a single plate. Thus, Hill's errors within a multiplet should be less than 10%.

If the relative strengths of the two chromium multiplets are computed from the data in table VII, the following ratios are found.

$\frac{a^7S-z^7P^0}{a^7S-y^7P^0}$	Atomic Beam	Hook	Hill	NBS
	.263	.292	.295	.303

This disagreement of the atomic beam results with those reported by the other workers was recognized, and scans of the six chromium lines were repeated. The relative strengths of the two multiplets found from the repeated work differed by less than 4% from the original values.

Table VIII. Relative f-Values within Multiplets

El.	$\lambda$	Multiplet	f(Th) (24)	f(AB)	f(NBS) (3)	f(hook)	f(Abs) (33)
Cr	4254	$a^7s_3-z^7P_4^0$	1.0	1.0	1.0	1.0 <sup>(12)</sup>	1.0
	4275	3- 3	.78	.77	.76	.73	.78
	4290	3- 2	.56	.58	.48	.55	.57
Cr	3579	$a^7s_3-y^7P_4^0$	1.0	1.0	1.0	1.0	1.0
	3593	3- 3	.78	.81	.87	.80	.78
	3605	3- 2	.56	.60	.61	.57	.60
In	4101	$5p^2P_{1/2}-5s^2S_{1/2}$	1.0	1.0	.71	1.0 <sup>(13)</sup>	
	4511	3/2- 1/2	.91	.92	1.0	1.08	
In	3039	$5p^2P_{1/2}-5d^2D_{3/2}$	1.0	1.0	1.0	1.0	
	3256	3/2- 5/2	.84	.85	1.0	1.01	
	3259	3/2- 3/2		.093	.09	.16	
Ga	4033	$4p^2P_{1/2}-4s^2S_{1/2}$	1.0	1.0	1.0	1.0 <sup>(13)</sup>	
	4172	3/2- 1/2	.97	1.06	.90	1.05	
Ga	2874	$4p^2P_{1/2}-4d^2D_{3/2}$	1.0	1.0	1.0	1.0	
	2943	3/2- 5/2	.88	.83	1.03	.91	
	2944	3/2- 3/2	.098	.097	.16	.12	

Table VIII. (Cont.)

El.	$\lambda$	Multiplet	f(Th) (24)	f(AB)	f(NBS) (3)	f(hook)	f(Abs)
Sn	2863	$5p^2 \ ^3P_0 - 6s \ ^3P_1^o$	1.0	1.0	1.0		
	2840	2-	2	.76	.62	.77	
	3009	1-	1	.24	.18	.28	
	3175	2-	1	.38	.33	.16	
	3034	1-	0	.31	.36	.31	
	2706	1-	2	.26	.44	.57	

C. Limitations of the Apparatus  
and Suggested Improvements

The atomic beam method of measuring absolute f-values appears to be a reliable one. The method can, in principle, be applied to any element which forms a monatomic gas.

The experimental techniques discussed in this thesis have the following limitations:

- 1) The high pressure mercury light source does not provide a usable continuum below 2650 Å.
- 2) The EMI, type 9526b, photomultiplier that was used for this work is not sensitive to wavelengths longer than 5500 Å.
- 3) The present vacuum system attains a pressure of about  $10^{-6}$  Torr while the furnace is hot. Elements which are known to getter, such as titanium and barium, would not deposit as pure metals at these pressures.
- 4) The photomultiplier scanner is not accurate for lines with equivalent widths less than .4 mA.
- 5) Deposit rates less than .03  $\mu\text{gm./sec.}$  are impossible to measure accurately because of the basic noise level in the microbalance.
- 6) Zirconia crucibles can not be used at temperatures above 2150 °C.
- 7) The assumption that the atomic beam effuses from the hole in the crucible with a mean free path larger than the size of the orifice means that the vapour pressure of

the metal atoms within the crucible should be kept below .1 Torr.

8) Absorption lines which arise from electronic levels populated with less than 5% of the atoms are generally too weak to produce equivalent widths greater than .4 mA<sup>0</sup>.

9) The thin walled graphite furnace tubes used for this experiment develop hot spots and burn out at temperatures above 2500 °C.

Some of these experimental limitations could be easily overcome; others would require major revisions of the equipment. Possibilities for improvement of the apparatus will be presented in the same respective order as the above stated limitations:

1) Light sources with sizable outputs below 2650 A<sup>0</sup> are probably available commercially. A high pressure hydrogen arc would be the first type of source to try.

2) Photomultipliers sensitive to wavelengths longer than 5500 A<sup>0</sup> are available commercially.

3) Modern vacuum techniques allow the attainment of pressures well below 10<sup>-9</sup> Torr. It would, however, be a large task to redesign the atomic beam furnace for use at such pressures because of the need to get cooling water, light, and electricity into the system and also to have it readily demountable.

4) The possibilities for improving the sensitivity of the present photomultiplier scanner have been explored rather thoroughly with no success. Perhaps the method now

being developed by Bell (37), in which the atomic beam is chopped in the vacuum chamber and a phase locked detector looks at the AC component in the transmitted light, is capable of greater sensitivity.

Bauch and Lomb has available a grating for the 21 ft. 10 in. spectrograph, which has 1200 rulings per mm. and about 16 cm. of rulings. This grating would allow an increase in resolution of about a factor of three above the present grating. Used in connection with the existing scanner, this grating should allow lines as small as  $.15 \text{ m}\mu$  in equivalent width, to be measured with roughly 10% accuracy.

The stationary wide slit method discussed on page 35 might prove to be more accurate than the existing scanner method if used in connection with the increased resolution available with the Bauch and Lomb grating. Errors due to non-constancy of the scanning speed could thus be eliminated.

5) A factor of at least two in effective microbalance sensitivity can be gained merely by increasing the size of the hole which allows the atomic beam to deposit on the balance pan. Pans large enough to cover a hole .8 in. in diameter should not overload the microbalance.

6) Magnesia, beryllia, and tantalum carbide crucibles can be heated to higher temperatures than stabilized zirconia and have about the same degree of chemical inactivity. These crucibles could be heated in tantalum furnace tubes, which should be able to reach  $2500^\circ \text{C}$  without burning out. Another possibility would be to use sintered tungsten

crucibles, constructed in such a way as to avoid shorting out the furnace current.

7) A multiple reflection mirror system, with the mirrors mounted inside the vacuum chamber, would allow lines with  $f$ -values below .01 to be studied, without resorting to unduly high beam densities. The only drawback would be the loss in light intensity.

8) Further work on very weak lines arising from lowly populated electronic levels could be done, once the range of measureable equivalent widths was extended to .15  $\text{m}\text{\AA}$ .

9) Heating by induction or by electron bombardment would probably be superior to the present furnace for attaining temperatures above 2500  $^{\circ}\text{C}$ .

D. Suggestions for Further Research

A brief discussion will follow of the possibilities for using the atomic beam method to measure the f-values for resonance lines of elements other than those on which some work has already been done.

Scandium, yttrium and the rare earths should form atomic beams at temperatures around 2000 °C. They all form carbides so it would probably be necessary to use zirconia crucibles. The most serious problem in the study of these elements would be their chemical activity. At  $10^{-6}$  Torr the amount of gettering which would occur on the micro-balance pan might make accurate determination of atomic beam densities impossible.

Titanium, which is a well known getter, is probably impossible to study without going to residual vacuum pressures below  $10^{-8}$  Torr.

Vanadium has been found to form an atomic beam from a zirconia crucible at about 2000 °C. If adequate beam densities for observation of its resonance lines can be obtained before the zirconia melts, vanadium should be measurable with the present apparatus.

The strong resonance lines of zinc and cadmium could be studied if a good continuum source for wavelengths below 2500 Å were obtained. It would be necessary to measure crucible temperatures with a thermocouple.

Silicon has all its strong resonance lines below

2550 A°. Silicon is known to form various polyatomic vapour species (38) which would make the determination of the fraction of the atoms in the monatomic state very difficult.

Germanium also forms polyatomic vapours (38). It has one resonance line,  $\lambda_{2651}$ , which might be studied with the present light source. Graphite crucibles might be useable for vapourizing germanium.

Aluminum is particularly difficult to contain in the liquid state. It was found to react with zirconia, graphite, and quartz crucibles. An atomic beam of aluminum was produced from a recrystallized alumina crucible, but examination of the impulse forces indicated that the atomic beam was not pure aluminum but contained a sizable fraction of heavier molecules such as AlO or Al<sub>2</sub>O. There is some hope that tantalum carbide or sintered tungsten crucibles will solve this difficulty. If an atomic beam of aluminum could be produced it should present no other serious experimental difficulties.

Calcium and magnesium are of considerable interest both theoretically and astrophysically. However the chemical activity of these elements might make accurate atomic beam density measurements at residual gas pressures of  $10^{-6}$  Torr impossible.

REFERENCES

- (1) Unsöld, A. 1955, Physik der Sternatmosphären (2nd ed. ; Berlin : Springer-Verlag), pp.267-370
- (2) Glennon, B. M. and Wiese, W. L. 1962, Bibliography on Atomic Transition Probabilities (National Bureau of Standards Monograph #50).
- (3) Corliss, C. H. and Bozman, W. R. 1962, Experimental Transition Probabilities of Spectral Lines of Seventy Elements (National Bureau of Standards Monograph #53).
- (4) Ottinger, C. and Ziock, K. 1961, Z. Naturforsch., 16a, 720.
- (5) Demtroder, W. 1962, Z. f. Physik, 166, 42.
- (6) King, R. B. and King, A. S. 1935, Ap. J., 82, 377.
- (7) King, R. B. and King, A. S. 1938, Ap. J., 87, 24.
- (8) King, R. B. and Stockbarger, D. C. 1940, Ap. J., 91, 488.
- (9) Estabrook, F. B. 1951, Ap. J., 113, 684.
- (10) Estabrook, F. B. 1952, Ap. J., 115, 571L.
- (11) Optical Transition Probabilities, A Collection of Russian Articles, 1924-1960, translated from Russian. Published for the National Science Foundation, Washington, D.C. and the Department of Commerce, U.S.A. by the Israel Program for Scientific Translations, 1962.
- (12) Ostrovskii, Yu. I. and Penkin, N. P. 1957, Optika i Spektroskopiya, 3, 193.
- (13) Ostrovskii et al. 1958, Optika i Spektroskopiya, 4, 719.
- (14) Wessel, G. 1949, Z. f. Physik, 126, 440.
- (15) Kopfermann, H. and Wessel, G. 1959, Z. f. Physik, 130, 100.
- (16) Davis, M. H. 1955, Thesis (Calif. Inst. of Tech.).
- (17) Bell, G. D. 1957, Thesis (Calif. Inst. of Tech.).
- (18) Bell, G. D., Davis, M. H., King, R. B., and Routly, P. M. 1958, Ap. J., 127, 775.
- (19) Bell et al. 1959, Ap. J., 129, 437.

- (20) Bell, G. D. and King, R. B. 1961, Ap. J., 133, 718.
- (21) Lawrence, G. M. 1963, Thesis (Calif. Inst. of Tech.).
- (22) Aller, L. H. 1953, Astrophysics, V. 1 (1st ed.; New York: Ronald Press Co.).
- (23) Landolt-Bornstein 1952, Zahlenwerte u. Funktionen, I Band, 5 Teil (Berlin: Springer-Verlag), pp. 1-63.
- (24) White, H. E. and Eliason, A. Y. 1933, Phys. Rev., 44, 753.
- (25) Stull, D. R. and Sinke, G. C. 1956, Thermodynamic Properties of the Elements, (Washington, D. C.: Am. Chem. Soc.).
- (26) Kuhn, H. G. 1962, Atomic Spectra (1st ed.; New York: Academic Press), p. 190.
- (27) Vonwiler, O. 1930, Phys. Rev., 35, 802.
- (28) Kvater, G. S. 1941, ZhETF, 11, 421.
- (29) Speiser, R., Johnston, H. L. and Blackburn, P. 1950, J. Am. Chem. Soc., 72, 4142.
- (30) Allen, C. W. and Assad, A. S. 1957, Monthly Notices Roy. Astron. Soc., 177, 35.
- (31) Allen, C. W. 1957, Monthly Notices Roy. Astron. Soc. 117, 622.
- (32) Allen, C. W. 1960, Monthly Notices Roy. Astron. Soc. 121, 299.
- (33) Hill, A. J. and King, R. B. 1951, J. Optical Soc. Am., 41, 315.
- (34) Goldberg, L., Muller, E. A. and Aller, L. H. 1960, Ap. J. Suppl., 45, 1-138.
- (35) Moise, N. 1963, Thesis (Calif. Inst. of Tech.).
- (36) Gurvich, L. V. 1958, Optika i Spektroskopiya, 5(2), 205.
- (37) Bell, G. D. 1962, Verbal communication based on research in progress, Harvey Mudd College, Claremont, Calif.
- (38) Honig, R. E. 1954, J. Chem. Phys., 22, 1610.